

Supporting Information

Coordination-Induced N–H Bond Weakening in a Molybdenum Pyrrolidine Complex: Isotopic Labeling Provides Insight into the Pathway for H₂ Evolution

*Máté J. Bezdek, István Pelczer and Paul J. Chirik**

*Department of Chemistry, Frick Laboratory
Princeton University, Princeton, NJ 08544, USA*

pchirik@princeton.edu

Table of Contents

I.	General Considerations	S2
II.	Preparation of Molybdenum Complexes	S5
III.	Preparation of Pyrrolidine Isotopologs	S8
IV.	Deuterium Labeling Experiments and Associated Data	S13
V.	Additional Reactions and Associated NMR Data	S35
VI.	Additional Spectroscopic Data	S38
	VI. A. EPR Spectra	S38
	VI. B. IR Spectra	S40
VII.	Electrochemical Determination of k_{PT} between [1-N(pyrr)] and [TBD–H][BArF²⁴]	S41
VIII.	DFT Input Examples	S42
	VIII. A. Geometry Optimizations	S42
	VIII. B. Numerical Frequency Calculations	S43
IX.	DFT-Computed Energies of Complexes	S44
X.	References	S45

I. General Considerations

All air- and moisture-sensitive manipulations were carried out using vacuum line, Schlenk and cannula techniques or in an MBraun inert atmosphere (nitrogen) dry box unless otherwise noted. The solvents used for air- and moisture-sensitive manipulations were dried and deoxygenated using literature procedures.¹ Celite was dried at 180 °C under vacuum for 3 days prior to use. Deuterium gas was purchased from Cambridge Isotope Labs (>99.8% purity), and passed through a column of MnO₂ supported on vermiculite and 3 Å molecular sieves prior to use on a Schlenk manifold. Deuterated solvents for NMR spectroscopy were distilled from sodium metal under an atmosphere of argon and stored over 4 Å molecular sieves. Pyrrolidine was purchased from Sigma-Aldrich, vacuum distilled from CaH₂ and stored over 4 Å molecular sieves. TBD (1,5,7-Triazabicyclo[4.4.0]dec-5-ene) was purchased from Sigma-Aldrich, dried under high vacuum and used without further purification. HCl (2.0 M in Et₂O) was purchased from Sigma-Aldrich and used as received. The following compounds were prepared according to literature procedures: **[1-CI]**,² Na[BArF²⁴],³ 2,4,6-tri-tert-butylphenoxy radical (*t*Bu₃ArO•),⁴ pyrrolidine-1-*d*₁,⁵ and [TBD-H][BArF²⁴].⁶

¹H NMR spectra were recorded on a Bruker AVANCE 500 spectrometer operating at 500.46 MHz. ¹³C NMR spectra were recorded on a 500 spectrometer operating at 125.85 MHz. ³¹P NMR spectra were collected on a 500 AVANCE spectrometers operating at 202.40 MHz, and were referenced to 85% H₃PO₄ as an external standard. ¹⁹F NMR spectra were collected on a Bruker 400 AVANCE spectrometer operating at 376.15 MHz and were referenced to CFCI₃ as an external standard. All ¹H and ¹³C NMR chemical shifts are reported in ppm relative to SiMe₄ using the ¹H (benzene-*d*₆: 7.16 ppm) and ¹³C (benzene-*d*₆: 128.06 ppm) chemical shifts of the solvent as a standard. ¹H NMR data for diamagnetic compounds are reported as follows: chemical shift, multiplicity (s = singlet, d = doublet, t = triplet, q = quartet, p = pentet, br = broad,

m = multiplet, app = apparent, obsc = obscured), coupling constants (Hz), integration, assignment.

Elemental analyses were performed at Robinson Microlit Laboratories, Inc., in Ledgewood, NJ. High-resolution mass spectra were obtained on an Agilent 7200 gas chromatography/mass spectrometry system using electron impact time-of-flight (EI-TOF). Infrared spectroscopy was conducted on a Thermo-Nicolet iS10 FT-IR spectrometer calibrated with a polystyrene standard.

Gouy magnetic susceptibility balance measurements were performed with a Johnson Matthey instrument that was calibrated with $\text{HgCo}(\text{SCN})_4$. Continuous wave EPR spectra were recorded on an X-band Bruker EMXPlus spectrometer equipped with an EMX standard resonator and a Bruker PremiumX microwave bridge. The spectra were simulated using EasySpin for MATLAB.⁷

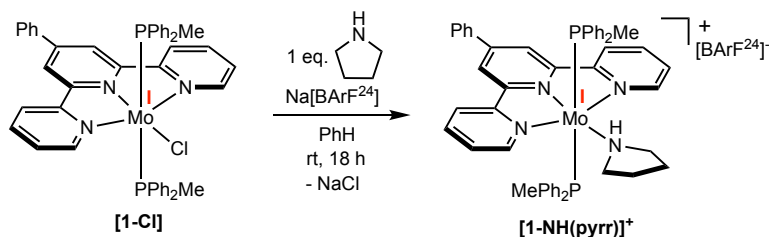
CVs were collected in THF solution (2 mM in compound) with $[(n\text{-Bu})_4\text{N}][\text{PF}_6]$ (0.2 M), using a 3 mm glassy carbon working electrode, platinum wire as the counter electrode, and silver wire as the reference in a drybox equipped with electrochemical outlets. CVs were recorded using a BASi EC Epsilon electrochemical workstation and analyzed using the BASi Epsilon-EC software. All CVs were run at 23 °C. Potentials are reported versus $\text{Cp}_2\text{Fe}/\text{Cp}_2\text{Fe}^+$ and were obtained using the *in situ* method.

All DFT calculations were performed with the ORCA program package in the gas phase.⁸ The geometry optimizations of the complexes and single-point calculations on the optimized geometries were carried out at the B3LYP level of DFT.⁹ The all-electron Gaussian basis sets were those developed by the Ahlrichs group.¹⁰ Triple- ζ quality basis sets def2-TZVP with one set of polarization functions on molybdenum, phosphorous and nitrogen were used. For the carbon and hydrogen atoms, slightly smaller polarized split-valence def2-SV(P) basis sets were used that were of double- ζ quality in the valence region and contained a polarizing set of d functions on the non-hydrogen atoms. Auxiliary basis sets to expand the electron density in the

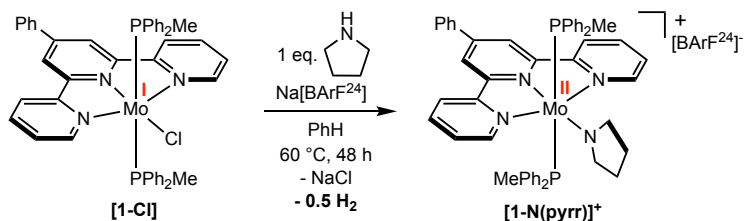
resolution-of-the-identity (RIJCOSX)¹¹ approach were chosen to match the orbital basis.¹² Numerical frequencies were calculated at the same level of theory to confirm the optimized geometries (no imaginary frequencies) and to derive thermochemical data. Bond dissociation free energies were computed at standard conditions of 1 atm and 25 °C including corrections for vibrational zero-point energy, as well as contributions from translational, rotational, and vibrational modes to the energy and entropy of the homolytic bond cleavage process. For molecules containing a molybdenum atom, the 0th order regular approximation (ZORA) was applied.¹³ In this case, the relevant basis sets were replaced by their relativistically recontracted versions.¹⁴ The electronic energy of H•, utilized in the calculation of bond dissociation free energies, at the present level of theory is 312 kcal/mol.

The supplemental file **om0c00471_si_001.xyz** contains the computed Cartesian coordinates of all of the molecules reported in this study. The file may be opened as a text file to read the coordinates, or opened directly by a molecular modeling program such as Mercury (version 3.3 or later, <http://www.ccdc.cam.ac.uk/pages/Home.aspx>) for visualization and analysis.

II. Preparation of Molybdenum Complexes

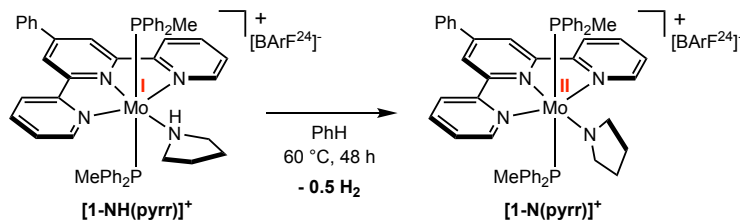


Preparation of [1-NH(pyrr)]⁺. In the glovebox, a J-Young NMR tube was charged with **[1-Cl]** (0.048 g, 0.057 mmol) and Na[BArF²⁴] (0.053 g, 0.060 mmol), pyrrolidine (0.005 mL, 0.060 mmol) and benzene (0.6 mL). The vessel was quickly sealed with a Teflon cap and connected to the high vacuum line where the mixture was de-gassed by 3x freeze-pump-thaw cycles. The tube was sealed and rotated end-over-end at room temperature for 18 hours. The tube was then brought back into the glovebox, where the mixture was filtered through a pad of Celite, and the solvent was removed *in vacuo*. The dark residue was washed with pentane (3 x 3 mL) and dried *in vacuo* to yield **[1-NH(pyrr)]⁺** as a dark green solid (0.084 g, 0.048 mmol, 85%). Anal Calcd for C₈₃H₆₂BF₂₄MoN₄P₂: C, 57.29; H, 3.59; N, 3.22. Found: C, 56.95; H, 3.58; N, 3.27. Magnetic Susceptibility (Guoy balance, 296 K): $\mu_{\text{eff}} = 1.7(2) \mu_{\text{B}}$. IR (KBr, 296 K, cm⁻¹): 3246 (NHpyrr), 2400 (NDpyrr). The isotopologue **[1-ND(pyrr)]⁺** was prepared in a manner similar to **[1-NH(pyrr)]⁺** with the exception that pyrrolidine-1-*d*₁ was used in place of pyrrolidine.



Preparation of [1-N(pyrr)]⁺ (Method A). In the glovebox, a 50 mL thick-walled glass vessel was charged with a magnetic stir bar, 0.194 g (0.231 mmol) of **[1-Cl]**, 0.215 g (0.242 mmol) of Na[BArF²⁴], 0.020 mL (0.240 mmol) of pyrrolidine and 3 mL of benzene. The vessel was quickly sealed with a Teflon valve and connected to the high vacuum line where the mixture was de-

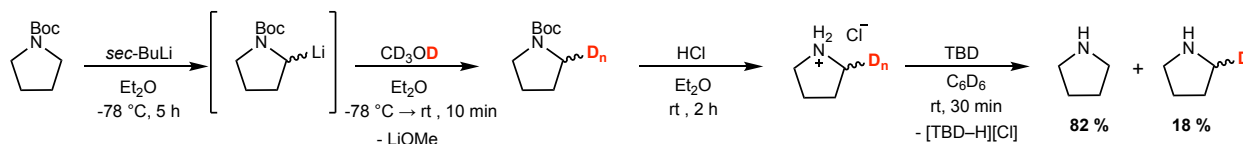
gassed by 3x freeze-pump-thaw cycles. The reaction vessel was then sealed and the mixture stirred at 60 °C under vacuum for 48 hours. Using a Toepler pump, 0.094 mmol (0.407 equivalents per Mo) of gas was collected. The gas was passed over a bed of CuO pre-heated to 200 °C. After this procedure, no gas was collected, confirming the identity of the evolved gas as H₂. The reaction vessel was then brought back into the glovebox and the mixture was filtered through a pad of Celite, followed by the removal of the solvent *in vacuo*. The dark residue was washed with pentane (3 x 3 mL) followed by trituration with pentane (5 x 5 mL) to yield the product as a dark brown solid (0.394 g, 0.227 mmol, 98%). Anal Calcd for C₈₃H₆₁BF₂₄MoN₄P₂: C, 57.32; H, 3.54; N, 3.22. Found: C, 57.06; H, 3.42; N, 3.15. ¹H NMR (benzene-*d*₆, 295 K): δ 8.92 (d, ³J_{C-H} = 6.1 Hz, 2H, ^{Ph}Tpy aryl-CH), 8.48 (s, 8H, B[(3,5-(CF₃)₂)C₆H₃]₄), overlap with 2H, ^{Ph}Tpy aryl-CH), 7.71 (s, 4H, B[(3,5-(CF₃)₂)C₆H₃]₄), 7.49 (br s, 2H, ^{Ph}Tpy aryl-CH), 7.48 (br s, 2H, ^{Ph}Tpy aryl-CH), 7.30 (br s, 1H, ^{Ph}Tpy aryl-CH), 7.25 (br s, 2H, ^{Ph}Tpy aryl-CH), 6.78 (t, ³J_{C-H} = 7.5 Hz, 4H, P(C₆H₅)₂(CH₃)), 6.64 (t, ³J_{C-H} = 7.7 Hz, 8H, P(C₆H₅)₂(CH₃)), 6.61 (d, ³J_{C-H} = 7.5 Hz, 2H, ^{Ph}Tpy aryl-CH), 6.51 (t, ³J_{C-H} = 6.6 Hz, 2H, ^{Ph}Tpy aryl-CH), 6.09 – 6.04 (m, 8H, P(C₆H₅)₂(CH₃)), 4.04 (br s, 4H, N(pyrr) α-CH₂), 1.75 (br s, 4H, N(pyrr) β-CH₂), 0.55 (s, 6H, P(C₆H₅)₂(CH₃)). ¹³C{¹H} NMR (benzene-*d*₆, 295 K): δ 162.88 (q, ¹J_{C-B} = 49.8 Hz, B[(3,5-(CF₃)₂)C₆H₃]₄), 146.12 (s, ^{Ph}Tpy aryl-C), 145.77 (s, ^{Ph}Tpy aryl-C), 139.62 (s, ^{Ph}Tpy aryl-C), 138.24 (s, ^{Ph}Tpy aryl-C), 136.41 (s, ^{Ph}Tpy aryl-C), 135.54 (s, B[(3,5-(CF₃)₂)C₆H₃]₄), 132.56 (app t, *J* = 16.0 Hz, P(C₆H₅)₂(CH₃)), 130.28 (app t, *J* = 5.5 Hz, P(C₆H₅)₂(CH₃)), 129.99 (q, ²J_{C-F} = 31.8 Hz, B[(3,5-(CF₃)₂)C₆H₃]₄), 129.45 (s, P(C₆H₅)₂(CH₃)), 129.35 (s, P(C₆H₅)₂(CH₃)), 129.03 (s, ^{Ph}Tpy aryl-C), 128.60 (s, ^{Ph}Tpy aryl-C), 128.54 (s, ^{Ph}Tpy aryl-C), 127.26 (s, ^{Ph}Tpy aryl-C), 125.35 (q, ¹J_{C-F} = 272 Hz, B[(3,5-(CF₃)₂)C₆H₃]₄), 122.65 (s, ^{Ph}Tpy aryl-C), 119.02 (s, ^{Ph}Tpy aryl-C), 118.18 (br s, B[(3,5-(CF₃)₂)C₆H₃]₄), 112.41 (s, ^{Ph}Tpy aryl-C), 71.44 (t, ³J_{C-P} = 11.6 Hz, N(pyrr) α-C), 26.75 (s, N(pyrr) β-C), 8.66 (app t, *J* = 9.2 Hz, P(C₆H₅)₂(CH₃)). ³¹P{¹H} NMR (benzene-*d*₆, 295 K): δ 11.95 (s).



Preparation of [1-N(pyrr)]⁺ (Method B). In the glovebox, a J-Young NMR tube fitted with a Teflon cap was charged with 0.050 g (0.029 mmol) of **[1-NH(pyrr)]⁺**, and 0.6 mL of benzene. The tube was sealed and connected to the high vacuum line where the solvent was de-gassed by 3x freeze-pump-thaw cycles.^A The tube was sealed and placed in a temperature-controlled oil bath (60 °C) for 48 hours. The tube was then brought back into the glovebox and product isolation was carried out as described in Method A to yield analytically pure **[1-N(pyrr)]⁺** as a dark brown solid (0.048 g, 0.028 mmol, 96 %).

^A It is important to degas the reaction mixture as pyrrolidine appears to be labile at elevated temperatures in the presence of N₂ to form the dimeric N₂ complex $\{[(\text{PhTpy})(\text{PPh}_2\text{Me})_2\text{Mo}]_2(\mu_2\text{-N}_2)\}[\text{BArF}_{24}]_2$.² The poor solubility of the dicationic complex in benzene causes precipitation of this side product and likely drives the reaction. In order to prevent the formation of this side product, the dehydrogenation can alternatively be carried out under an Ar atmosphere. However, in order to prevent pressure buildup in the closed vessel for larger scales, performing the reaction under vacuum was preferred.

III. Preparation of Pyrrolidine Isotopologs



Synthesis of pyrrolidine-2- d_7 . A literature report¹⁵ was modified. In the glovebox, a 100 mL 3-neck flask fitted with a Schlenk adapter was charged with a magnetic stir bar, and N-Boc-pyrrolidine (0.9 mL, 5.13 mmol) dissolved in 50 mL of Et₂O. The vessel was sealed and connected to the Schlenk line, where it was cooled to -78 °C. To the stirring solution, *sec*-BuLi (5 mL, 6.68 mmol, 1.35 M in cyclohexane) was added dropwise. The reaction was stirred at -78 °C for 5 hours, during which time the formation of a white precipitate was observed. After stirring for 5 hours, methanol- d_4 (0.417 mL, 10.27 mmol) was added dropwise and stirred for 10 minutes while warming to room temperature. The resulting suspension was then filtered through a pad of Celite, and solvent was removed *in vacuo* to yield N-Boc-pyrrolidine- d_n as a colorless oil (0.768 g, ~4.46 mmol, ~87 %).

Under open-air conditions, a 250 mL round-bottom flask was charged with N-Boc-pyrrolidine- d_n (0.8 mL, ~4.5 mmol) dissolved in 5 mL of Et₂O. To the stirring solution, HCl (3.4 mL, 13.6 mmol, 4.0 M in dioxane) was added dropwise. The mixture was stirred at room temperature for 2 hours. After this time, the solvent of the reaction was removed *in vacuo*. The residue was slightly oily and was washed with additional Et₂O (3 x 50 mL), dried *in vacuo*. The residue was additionally dried under high vacuum overnight and transferred to the glovebox. In the glovebox, the solids were isolated on a fine-porosity sintered glass frit, washed with pentane (3 x 10 mL) and dried *in vacuo* to yield pyrrolidine- d_n •HCl as a white solid. (0.300 g, ~ 2.76 mmol, ~61 %).

In the glovebox, a 20 mL scintillation vial was charged with a magnetic stir bar, pyrrolidine- d_n •HCl (0.006 g, ~0.058 mmol). To the stirring vial, a solution of TBD (0.024 g, 0.174 mmol) dissolved in 0.6 mL benzene- d_6 was added. The suspension was stirred for 15 minutes, the vial was tipped to wash the precipitates on the vial walls, and stirred again for 15 minutes. The mixture was then transferred to a 50 mL thick-walled glass vessel, sealed, connected to the high vacuum line where it was de-gassed via 3x freeze-pump-thaw cycles. The volatiles of the reaction mixture were then vacuum transferred to a J-Young NMR tube the isotopic composition of the liberated pyrrolidine was established by quantitative $^{13}\text{C}\{^1\text{H}\}$ NMR spectroscopy to be pyrrolidine (82 %) and pyrrolidine-2- d_1 (18 %).

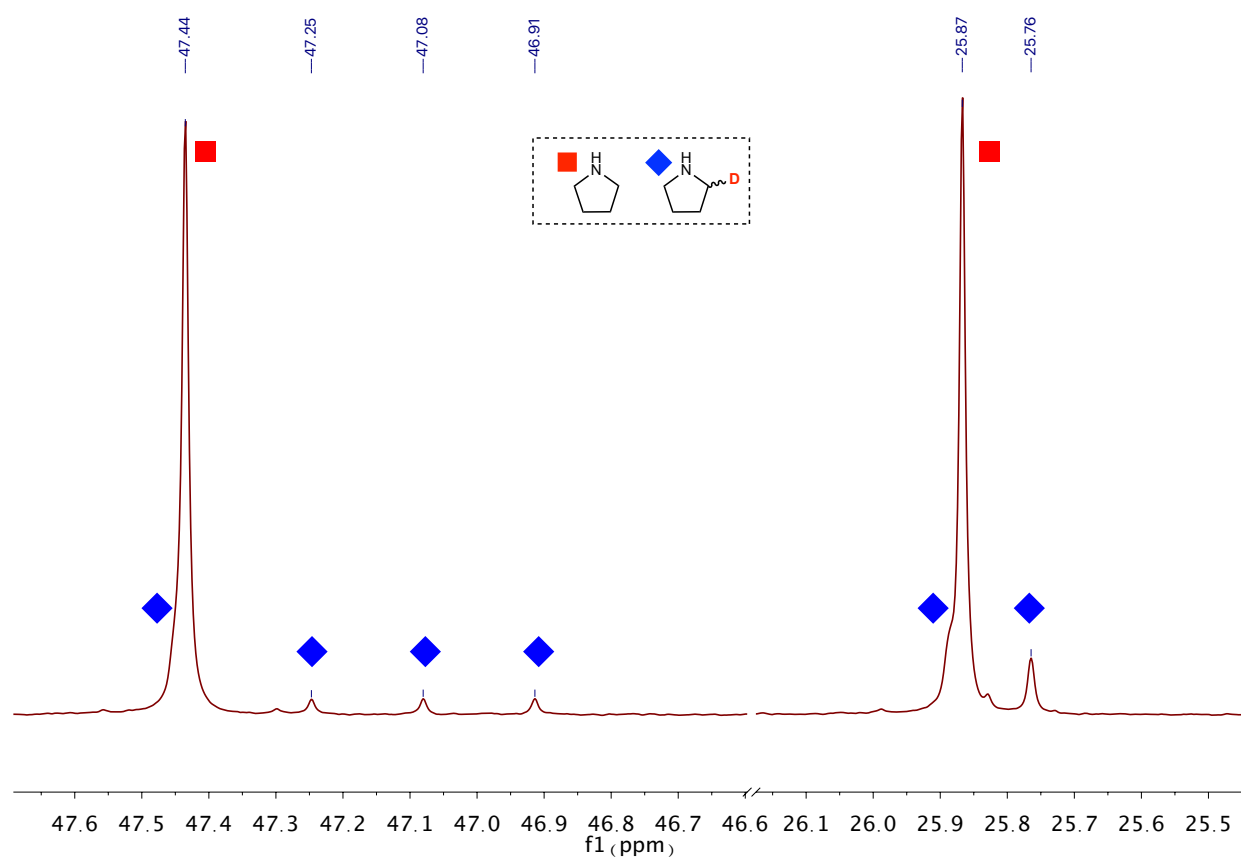
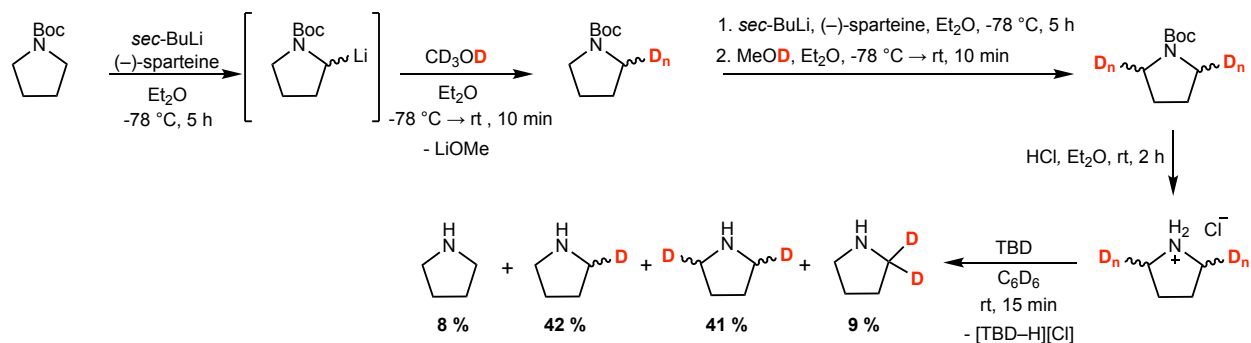


Figure S1. Quantitative $^{13}\text{C}\{^1\text{H}\}$ NMR spectrum (benzene- d_6 , 23 °C) of a mixture containing pyrrolidine (82 %) and pyrrolidine-2- d_1 (18 %) prepared by an independent route.



Synthesis of pyrrolidine-2,5-*d*₁, *d*₁, and pyrrolidine-2-*d*₂. A literature report¹⁵ was modified. In the glovebox, a 50 mL thick-walled glass vessel was charged with a magnetic stir bar and (-)-sparteine (0.875 g, 3.73 mmol) dissolved in 10 mL of Et₂O. A second 50 mL thick-walled glass vessel was charged with *sec*-BuLi (2.7 mL, 3.73 mmol, 1.39 M in cyclohexane). A third 200 mL thick-walled glass vessel was charged with a magnetic stir bar and N-Boc-pyrrolidine (0.5 mL, 2.87 mmol) dissolved in 25 mL of Et₂O. The three vessels were sealed with Teflon valves and connected to the Schlenk line, where the Teflon valves were replaced with rubber septa under a positive flow of Ar. Using a cannula, the *sec*-BuLi solution was added to the pre-cooled (-78 °C) sparteine solution and stirred at -78 °C for 15 minutes. After this time, the *sec*-BuLi/(-)-sparteine mixture was added to the pre-cooled (-78 °C) solution containing the N-Boc pyrrolidine via cannula. The resulting mixture was stirred at -78 °C for 5 hours. At the completion of the reaction, methanol-*d*₄ (0.24 mL) was added dropwise at -78 °C and the reaction mixture was warmed to room temperature over the course of 15 minutes. DI water (10 mL) was added to the mixture, and extracted with Et₂O (2 x 10 mL). The combined Et₂O fractions were then washed with 5% aqueous H₃PO₄ (20 mL), dried with MgSO₄ and filtered over Celite. Rotary evaporation of the solvent yielded N-Boc-pyrrolidine-*d_n* as a clear oil (0.442 g, ~2.57 mmol, 89 %). The product was de-gassed by 3x freeze-pump-thaw cycles, brought back into the glovebox where it was lyophilized from benzene (3 x 3 mL) and dried under vacuum for 1 hour. The labeling procedure was then repeated with the N-Boc-pyrrolidine-*d_n* thus obtained in order to generate

d_2 -isotopologs. Deprotection of the Boc group and subsequent deprotonation were carried out in analogy to the independent synthesis of pyrrolidine-2- d_1 described above. The isotopic composition of pyrrolidine was established by quantitative $^{13}\text{C}\{^1\text{H}\}$ NMR spectroscopy to be pyrrolidine (8 %) and pyrrolidine-2- d_1 (42 %), pyrrolidine-2,5- d_1,d_1 (41 %) and pyrrolidine-2- d_2 (9 %).

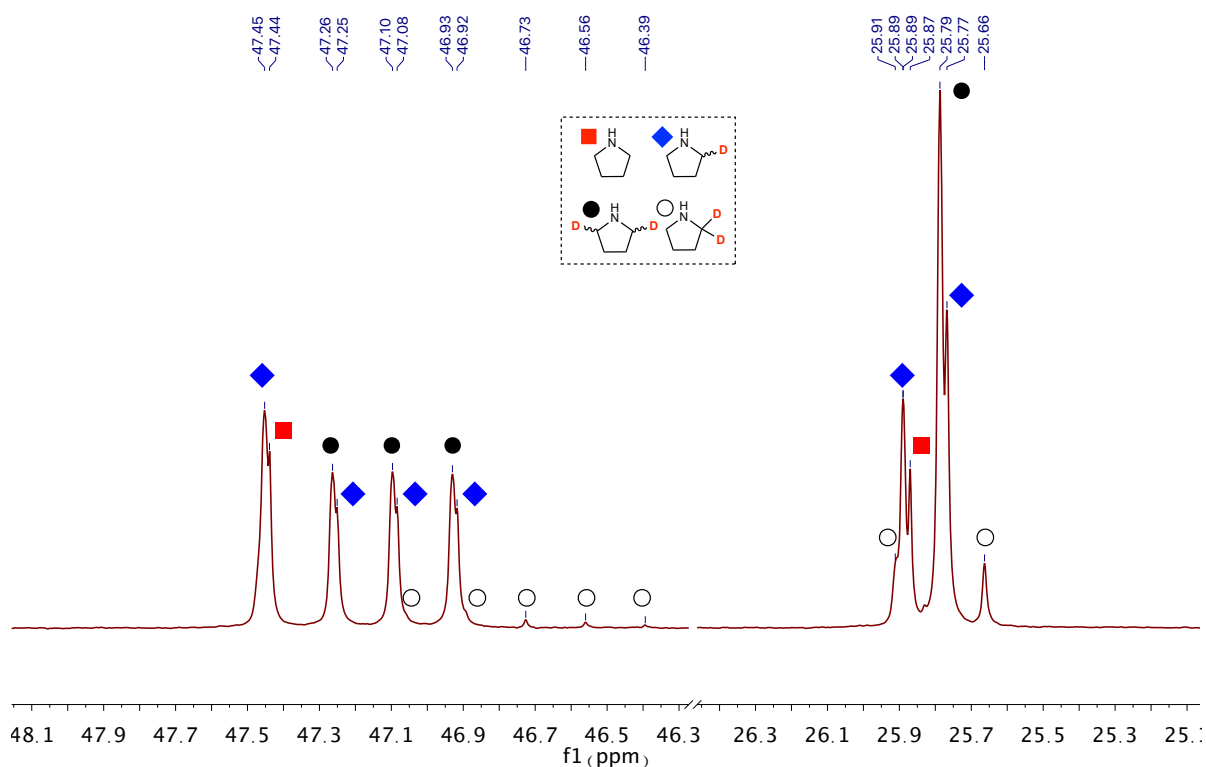


Figure S2. Quantitative $^{13}\text{C}\{^1\text{H}\}$ NMR spectrum (benzene- d_6 , 23 °C) of a mixture containing pyrrolidine (8 %) and pyrrolidine-2- d_1 (42 %), pyrrolidine-2,5- d_1,d_1 (41 %) and pyrrolidine-2- d_2 (9 %) prepared by an independent route.

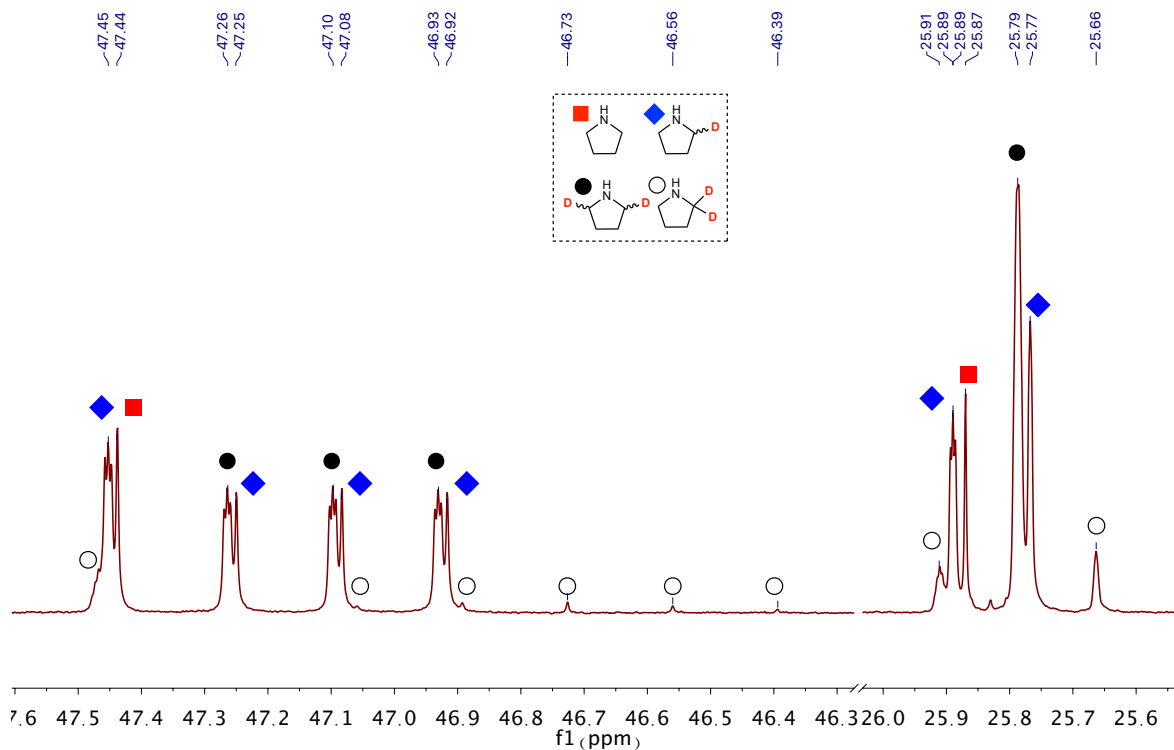
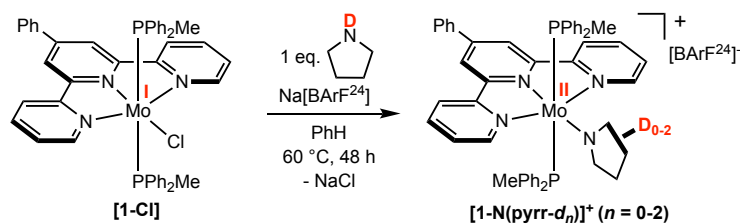
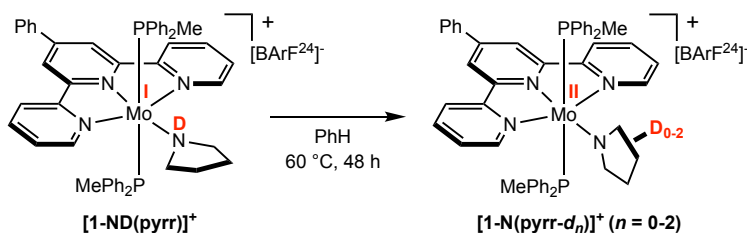


Figure S3. Quantitative $^{13}\text{C}\{^1\text{H}\}$ NMR spectrum (benzene- d_6 , 23 °C) of a mixture containing pyrrolidine (8 %) and pyrrolidine-2- d_1 (42 %), pyrrolidine-2,5- d_1,d_1 (41 %) and pyrrolidine-2- d_2 (9 %) prepared by an independent route. Data was processed with low exponential apodization (0.2 Hz).

IV. Deuterium Labeling Experiments and Associated Data



Preparation of [1-N(pyrr- d_n)]⁺ ($n = 0-2$) (Method A). In the glovebox, a 50 mL thick-walled glass vessel was charged with a magnetic stir bar, 0.200 g (0.238 mmol) of **[1-Cl]**, 0.221 g (0.250 mmol) of Na[BArF²⁴], 0.021 mL (0.250 mmol) of pyrrolidine- $N-d_1$ and 3 mL of benzene. The vessel was quickly sealed with a Teflon valve and connected to the high vacuum line where the mixture was de-gassed by 3x freeze-pump-thaw cycles. The reaction vessel was then sealed and the mixture stirred at 60 °C under vacuum for 48 hours. The reaction vessel was then brought back into the glovebox and product isolation was carried out as described for **[1-N(pyrr)]⁺** (Method A) to yield analytically pure **[1-N(pyrr- d_n)]⁺ ($n = 0-2$)** as a dark brown solid (0.404 g, 0.232 mmol, 98 %). ²H NMR (benzene, 295 K): δ 4.04 (br s, N(pyrr) α -CD).



Preparation of [1-N(pyrr- d_n)]⁺ ($n = 0-2$) (Method B). In the glovebox, a J-Young NMR tube fitted with a Teflon cap was charged with 0.050 g (0.029 mmol) of **[1-ND(pyrr)]⁺**, and 0.6 mL of benzene. The tube was sealed and connected to the high vacuum line where the solvent was de-gassed by 3x freeze-pump-thaw cycles. The tube was sealed and placed in a temperature-controlled oil bath (60 °C) for 48 hours. The tube was then brought back into the glovebox and product isolation was carried out as described for **[1-N(pyrr)]⁺** (Method A) to yield analytically

pure **[1-N(pyrr-*d*_{*n*})]⁺ (*n* = 0–2) as a dark brown solid (0.048 g, 0.028 mmol, 96 %). The isotopic composition of **[1-N(pyrr-*d*_{*n*})]⁺ (*n* = 0–2) was found to be independent of the method used for its preparation (A or B) as determined by ¹³C{¹H} NMR spectroscopic analysis of the liberated pyrrolidide ligand upon protonolysis (see below).****

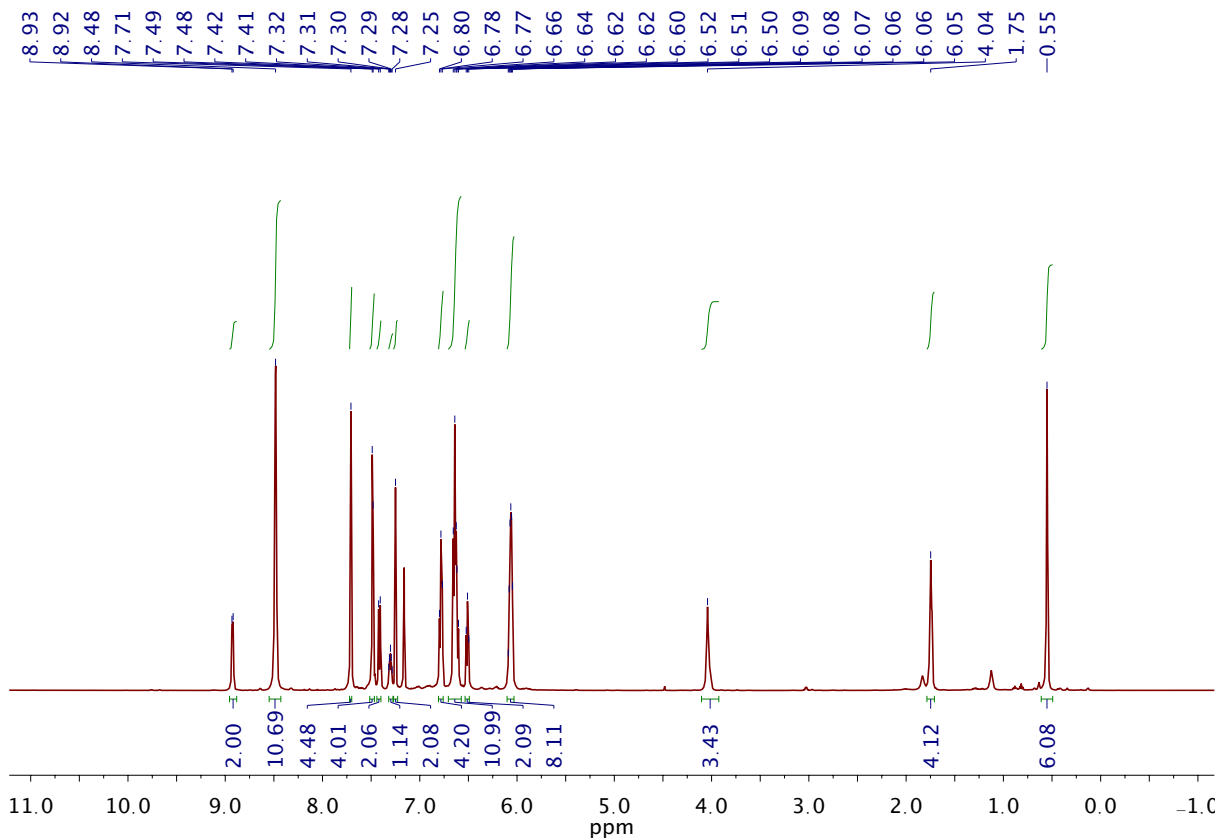


Figure S4. ¹H NMR (500 MHz) spectrum of **[1-N(pyrr-*d*_{*n*})]⁺ (*n* = 0, 1, 2) in benzene-*d*₆ at 23 °C. Note the low integration at the N(pyrr) α -CH₂ resonance compared to β -CH₂ (3.43 vs 4) that indicates deuteration at the α position, confirmed by ¹³C{¹H} NMR spectroscopy.**

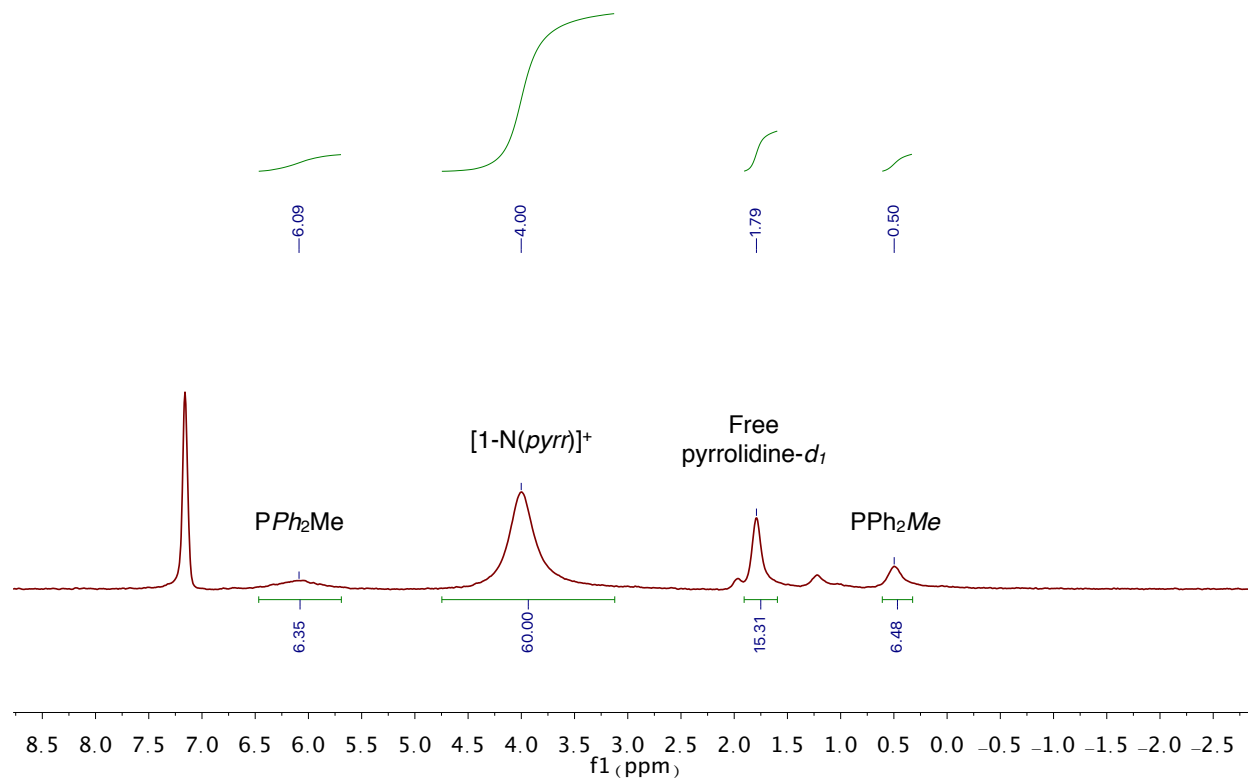
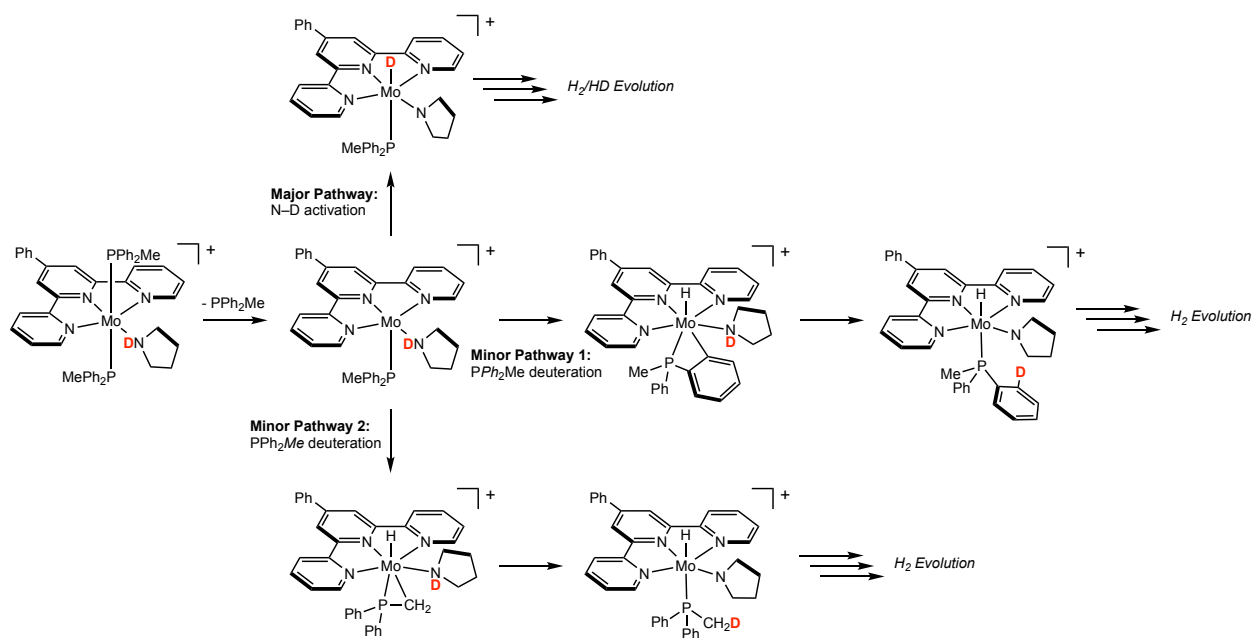
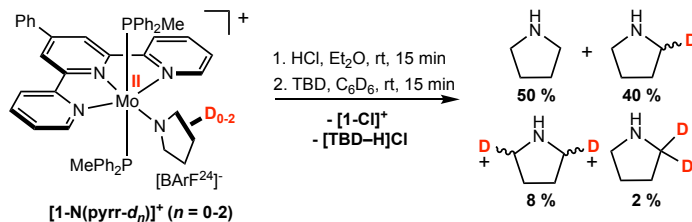


Figure S5. ^2H NMR spectrum (benzene, 23 °C) of the reaction mixture upon thermolysis of $[1\text{-ND}(\text{pyrr})]^+$, highlighting major deuterium incorporation into the pyrrolide ligand in $[1\text{-N}(\text{pyrr-d}_1)]^+$, with minor deuterium content in the PPh_2Me ligands.





Liberation of pyrrolidide ligand in $[1-N(\text{pyrr-}d_n)]^+$ ($n = 0-2$). In the glovebox, a 50 mL thick-walled glass vessel was charged with a magnetic stir bar, 0.078 g (~0.045 mmol) of $[1-N(\text{pyrr-}d_n)]^+$ (prepared via Method A or B) and dissolved in 1 mL of Et₂O. The vessel was sealed with a Teflon valve and connected to the high vacuum line where HCl (0.11 mL, 0.224 mmol, 2.0 M in Et₂O) was added via syringe under a positive flow of N₂. The mixture was stirred at room temperature for 15 minutes, during which time a color change from brown to green-brown was observed with the concomitant formation of precipitates. The mixture was de-gassed by 3x freeze-pump-thaw cycles and the solvent of the reaction was distilled away from the residue and ¹H NMR analysis of the residue indicated quantitative consumption of $[1-N(\text{pyrr-}d_n)]^+$ and formation of $[1-Cl]^+$. The residue was dried under high vacuum for 2 hours. After this time, the reaction vessel was brought back into the glovebox where 0.041 g (0.293 mmol) of TBD dissolved in 0.6 mL of benzene-*d*₆ was added. The vessel was sealed and mixture was stirred at room temperature for 15 minutes, followed by manual agitation of the reaction vessel to dissolve residue on side walls, followed by stirring at room temperature for an additional 15 minutes. The vessel was then connected to the high vacuum line and the volatiles were vacuum transferred to a J-Young NMR tube. The isotopic composition of the liberated pyrrolidone was established by quantitative ¹³C{¹H} NMR spectroscopy.

Liberation of pyrrolidide ligand in $[1-N(\text{pyrr})]^+$ with DCl (control experiment). The procedure described above was repeated with the exception that $[1-N(\text{pyrr})]^+$ was used in place of $[1-N(\text{pyrr-}d_n)]^+$ and DCl in place of HCl. ¹³C{¹H} NMR spectroscopy ruled out deuterium incorporation into the pyrrolidone backbone.

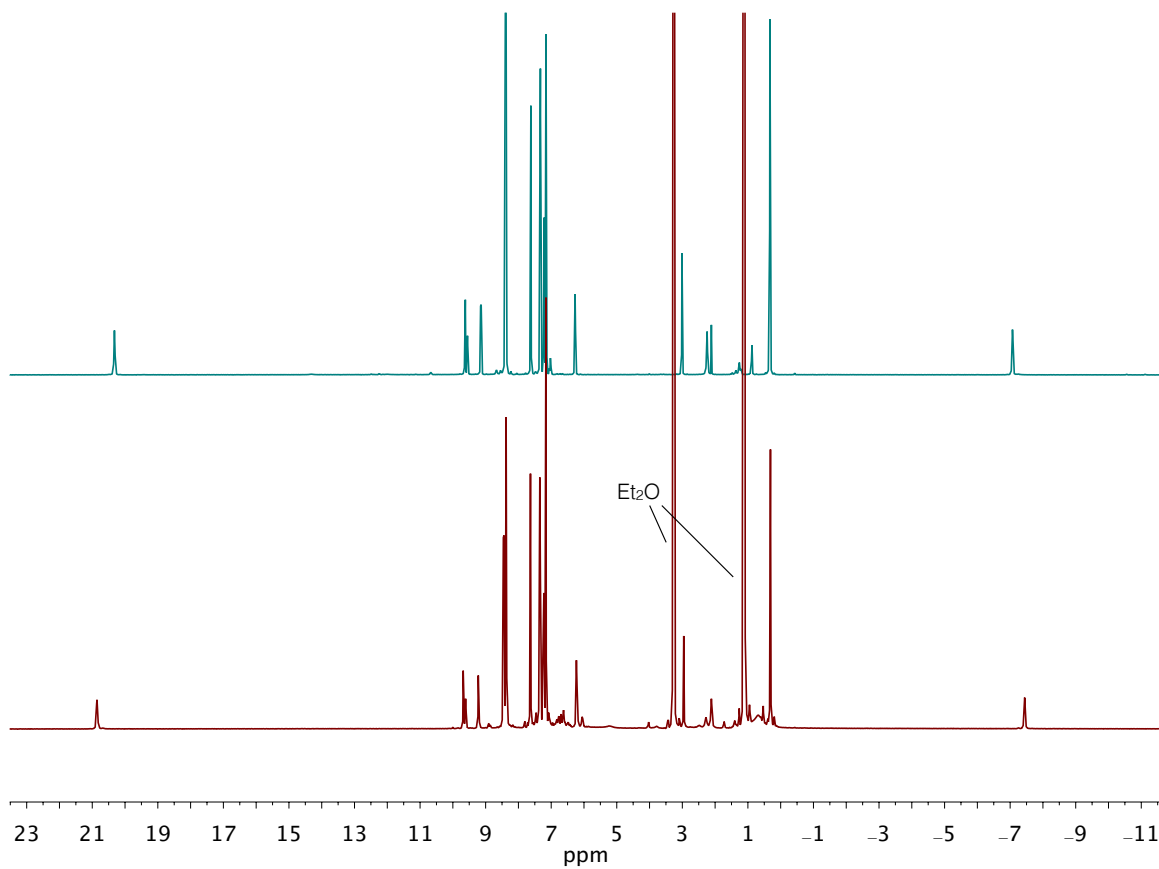


Figure S6. ¹H NMR (500 MHz) spectrum of the non-volatile residue upon treatment of **[1-N(pyrr-*d*_n)]⁺** (n = 0, 1, 2) with HCl (bottom) overlaid with an authentic sample containing **[1-Cl]⁺** (top)¹⁶ in benzene-*d*₆ at 23 °C .

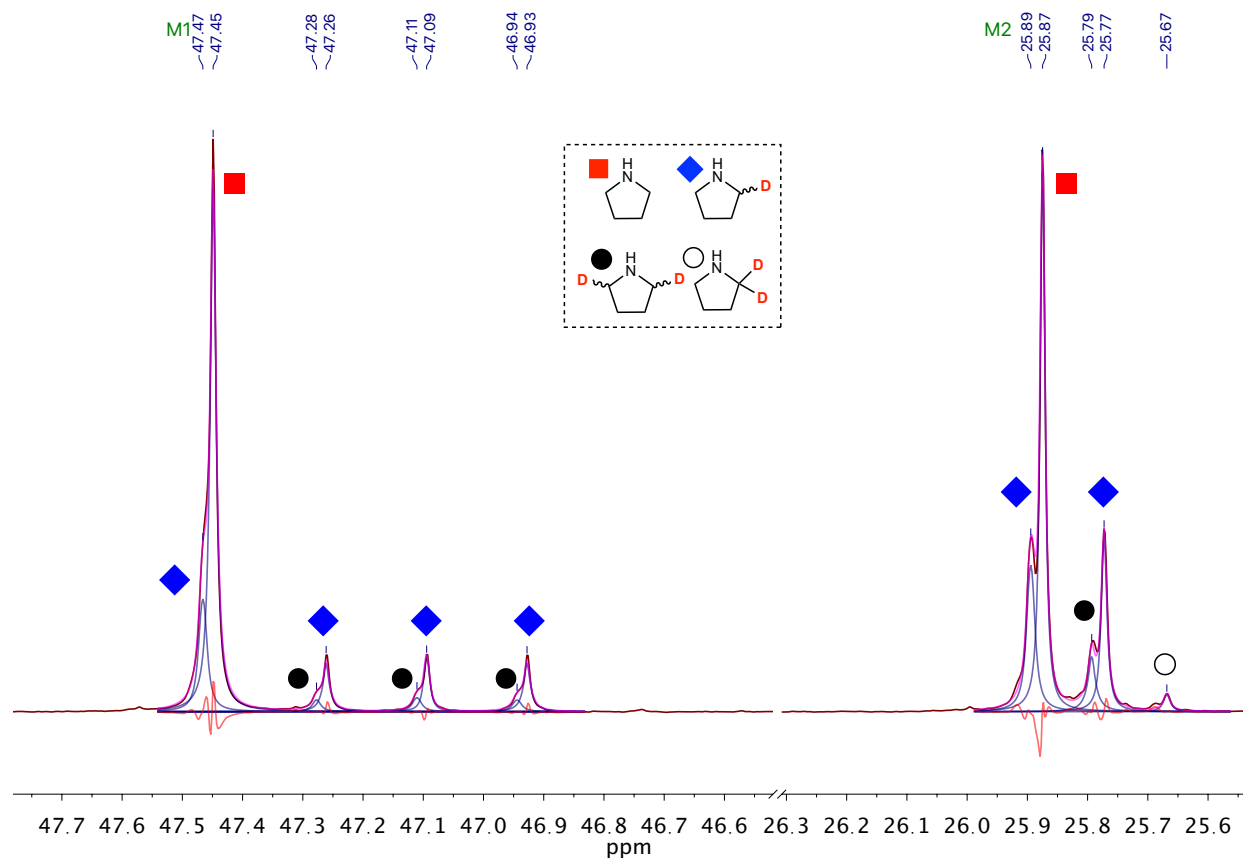
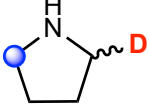
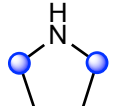
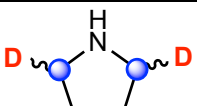
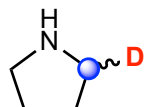
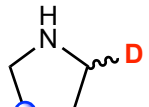
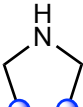
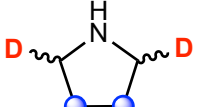
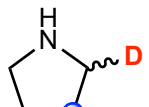
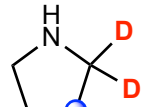


Figure S7. Fitted quantitative $^{13}\text{C}\{^1\text{H}\}$ NMR spectrum (benzene- d_6 , 23 °C) of a mixture containing pyrrolidine (50 %), pyrrolidine-2- d_1 (40 %), pyrrolidine-2,5- d_1,d_1 (8 %) and pyrrolidine-2,2- d_2 (2 %) liberated from $[(1\text{-N}(\text{pyrr-}d_n)]^+$ by protonolysis. The violet line represents a fit of the data, and the blue lines shows the deconvolution of the individual peaks.

Table S1. Assignments and relative integrations of the peaks observed in Figure S6.

δ (multiplicity)	Assignment	Integration (MestReNova Curve Fit)
47.47 (s)		121665.891
47.45 (s)		428855.552
47.28, 47.11, 46.94 (t, $^1J_{C-D} = 21$ Hz)		44800.913
47.26, 47.09, 46.93 (t, $^1J_{C-D} = 21$ Hz)		134666.055
25.89 (s)		157955.208 ^a
25.87 (s)		363337.345 ^a
25.79 (s)		59207.75 ^a
25.77 (s)		133826.336 ^a
25.67 (s)		15790.918 ^a

^a Values used to determine product percentages due to favorable peak deconvolution.

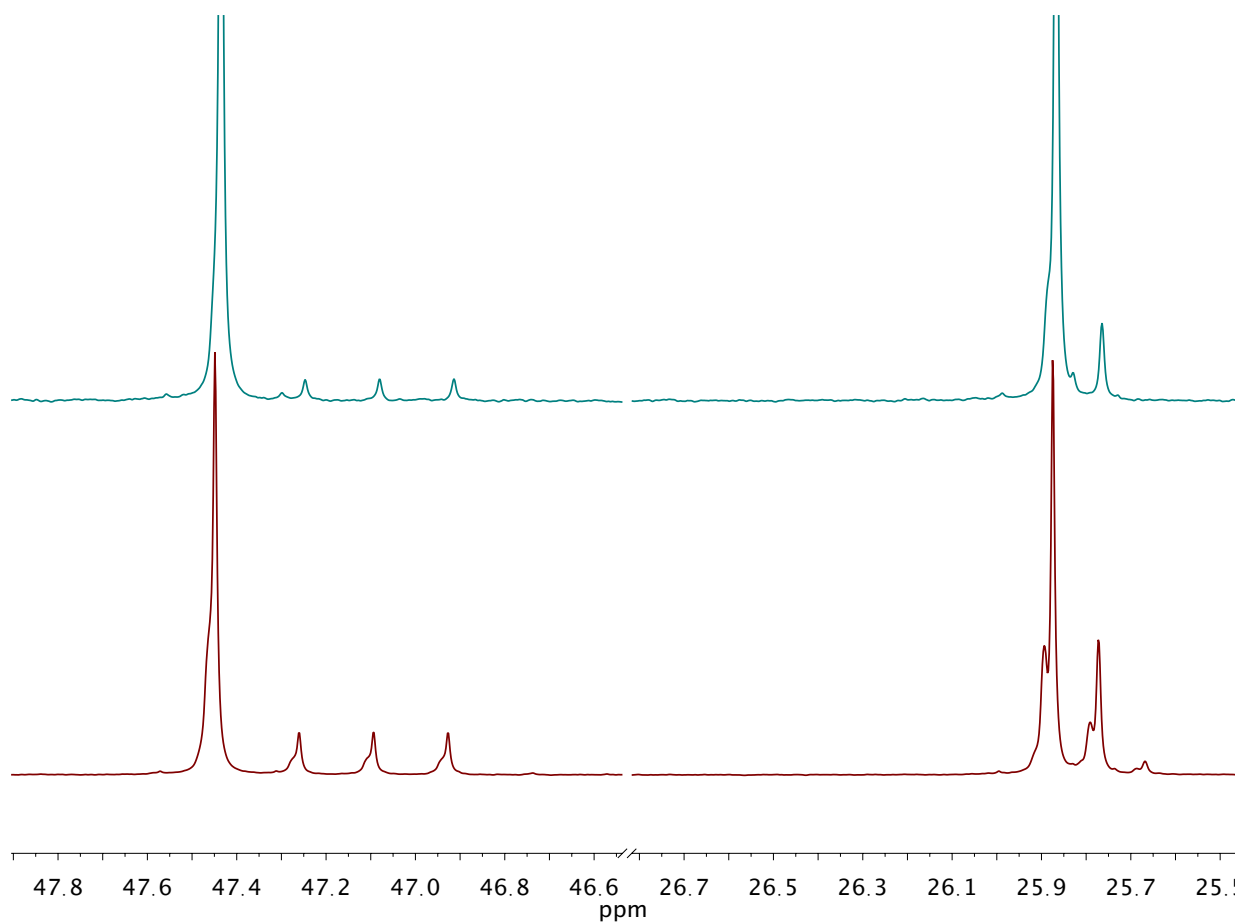


Figure S8. Quantitative $^{13}\text{C}\{^1\text{H}\}$ NMR spectrum (benzene- d_6 , 23 °C) of a mixture containing pyrrolidine (50 %), pyrrolidine-2- d_1 (40 %), pyrrolidine-2,4- d_2 (8 %) and pyrrolidine-2,2- d_2 (2 %) liberated from $[(1\text{-N}(\text{pyrr-}d_n)]^+$ by protonolysis (bottom, magenta), overlaid with an independently prepared mixture containing pyrrolidine (78 %) and pyrrolidine-2- d_1 (18 %) (top, blue). This spectrum supports the chemical shift assignment for pyrrolidine-2- d_1 as the major isotopolog present upon the liberation of the pyrrolidide ligand in $[(1\text{-N}(\text{pyrr-}d_n)]^+$.

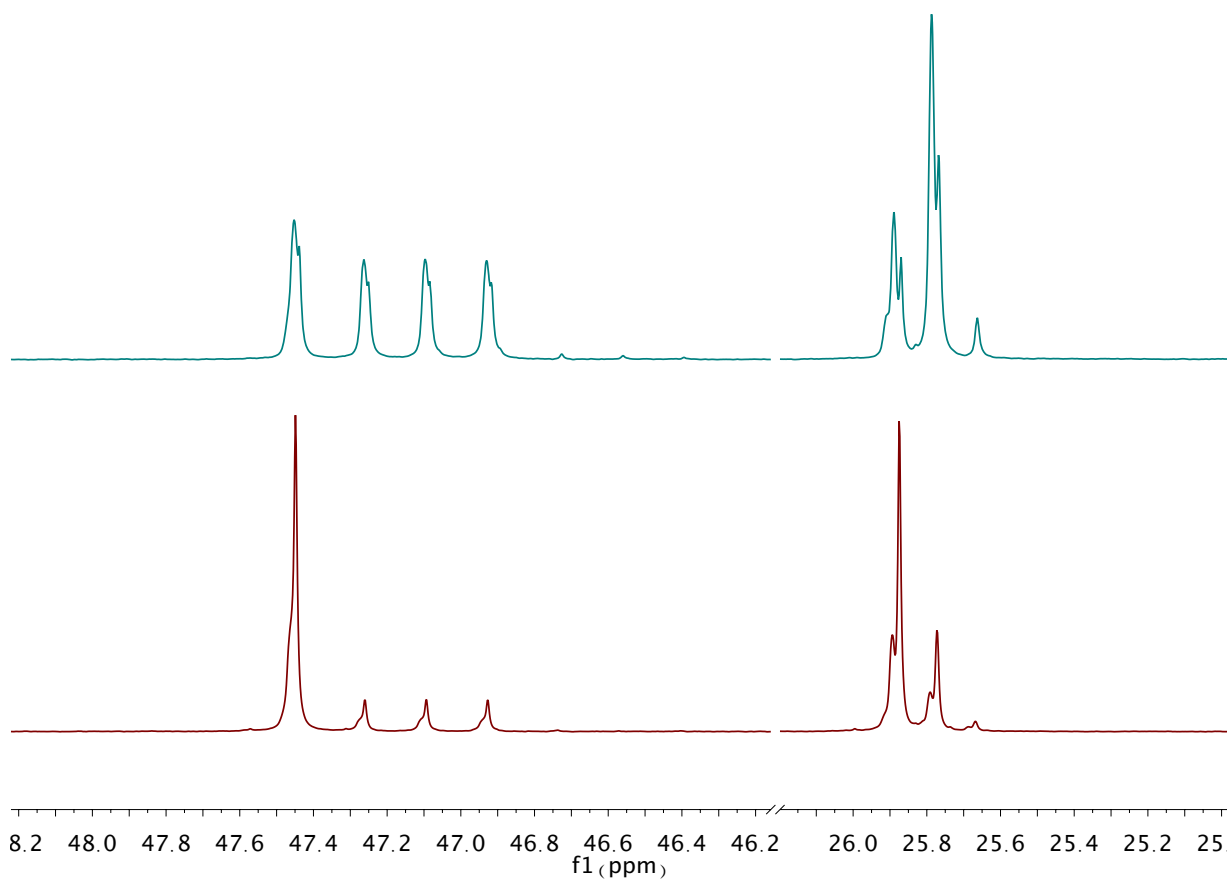


Figure S9. Quantitative $^{13}\text{C}\{^1\text{H}\}$ NMR spectrum (benzene- d_6 , 23 °C) of a mixture containing pyrrolidine (50 %), pyrrolidine-2- d_1 (40 %), pyrrolidine-2,5- d_1,d_1 (8 %) and pyrrolidine-2,2- d_2 (2 %) liberated from **[(1-N(pyrr- d_n)] $^+$** by protonolysis (bottom, magenta), overlaid with an independently prepared mixture containing pyrrolidine (8 %), pyrrolidine-2- d_1 (42 %), pyrrolidine-2,5- d_1,d_1 (41 %) and pyrrolidine-2,2- d_2 (9 %) (top, blue). This spectrum supports the chemical shift assignment for pyrrolidine isotopomers and isotopologs present upon the liberation of the pyrrolidide ligand in **[(1-N(pyrr- d_n)] $^+$** .

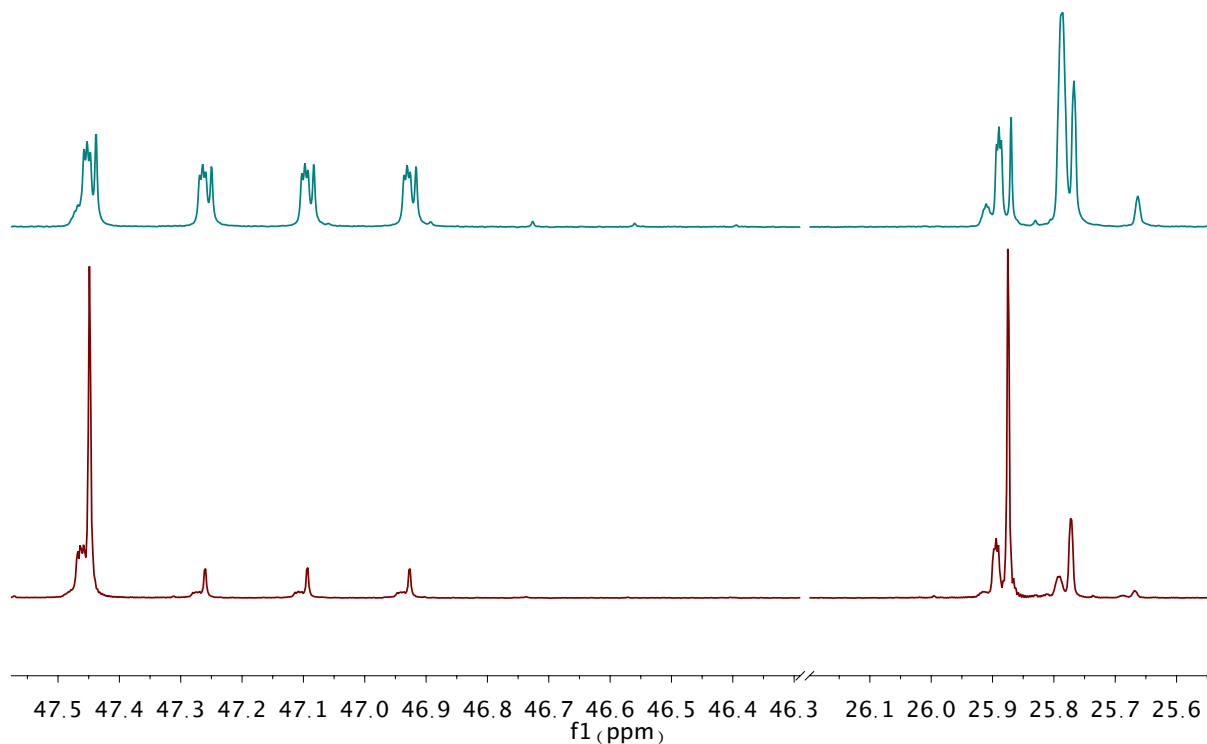
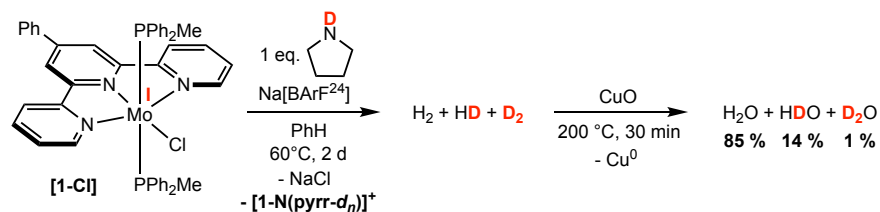


Figure S10. Quantitative $^{13}\text{C}\{^1\text{H}\}$ NMR spectrum (benzene- d_6 , 23 °C) of a mixture containing pyrrolidine (50 %), pyrrolidine-2- d_1 (40 %), pyrrolidine-2,5- d_1,d_1 (8 %) and pyrrolidine-2,2- d_2 (2 %) liberated from **[(1-N(pyrr- d_n)] $^+$** by protonolysis (bottom, magenta), overlaid with an independently prepared mixture containing pyrrolidine (8 %), pyrrolidine-2- d_1 (42 %), pyrrolidine-2,5- d_1,d_1 (41 %) and pyrrolidine-2,2- d_2 (9 %) (top, blue). This spectrum supports the chemical shift assignment for pyrrolidine isotopomers and isotopologs present upon the liberation of the pyrrolidide ligand in **[(1-N(pyrr- d_n)] $^+$** . Data was processed with low exponential apodization (0.2 Hz) to better resolve isotopolog/isotopomer peaks.



Figure S11. Mass spectrum of pyrrolidine (bottom), overlaid with a mixture containing pyrrolidine (50 %), pyrrolidine-2-*d*₁ (40 %), pyrrolidine-2,5-*d*₁,*d*₁ (8 %) and pyrrolidine-2,2-*d*₂ (2 %) liberated from [(1-N(pyrrolid-*d*_n)]⁺ by protonolysis (top).



Quantification of H₂ isotopologs formed during dehydrogenation of pyrrolidine-N-*d*₁. In the glovebox, a 50 mL thick-walled glass vessel was charged with a magnetic stir bar, 0.200 g (0.238 mmol) of **[1-Cl]**, 0.221 g (0.250 mmol) of Na[BArF²⁴], 0.021 mL (0.250 mmol) of pyrrolidine-N-*d*₁ and 3 mL of benzene. The vessel was quickly sealed with a Teflon valve and connected to the high vacuum line where the mixture was de-gassed by 3x freeze-pump-thaw cycles. The reaction vessel was then sealed and the mixture stirred at 60 °C under vacuum for 48 hours. After this time, using a Toepler pump, 0.094 mmol (0.407 equivalents per Mo) of gas was collected. The gas was passed over a bed of CuO pre-heated to 200 °C, and the combustion product was collected in a liquid nitrogen-cooled trap. The contents of the trap were then vacuum transferred to a J-Young NMR tube containing benzene-*d*₆ (0.6 mL) and analyzed by ¹H NMR spectroscopy. The relative amounts of H₂O, HDO and D₂O thus formed were calculated from the ratio of [H₂O]:[HDO] observed by ¹H NMR and the relation:¹⁷



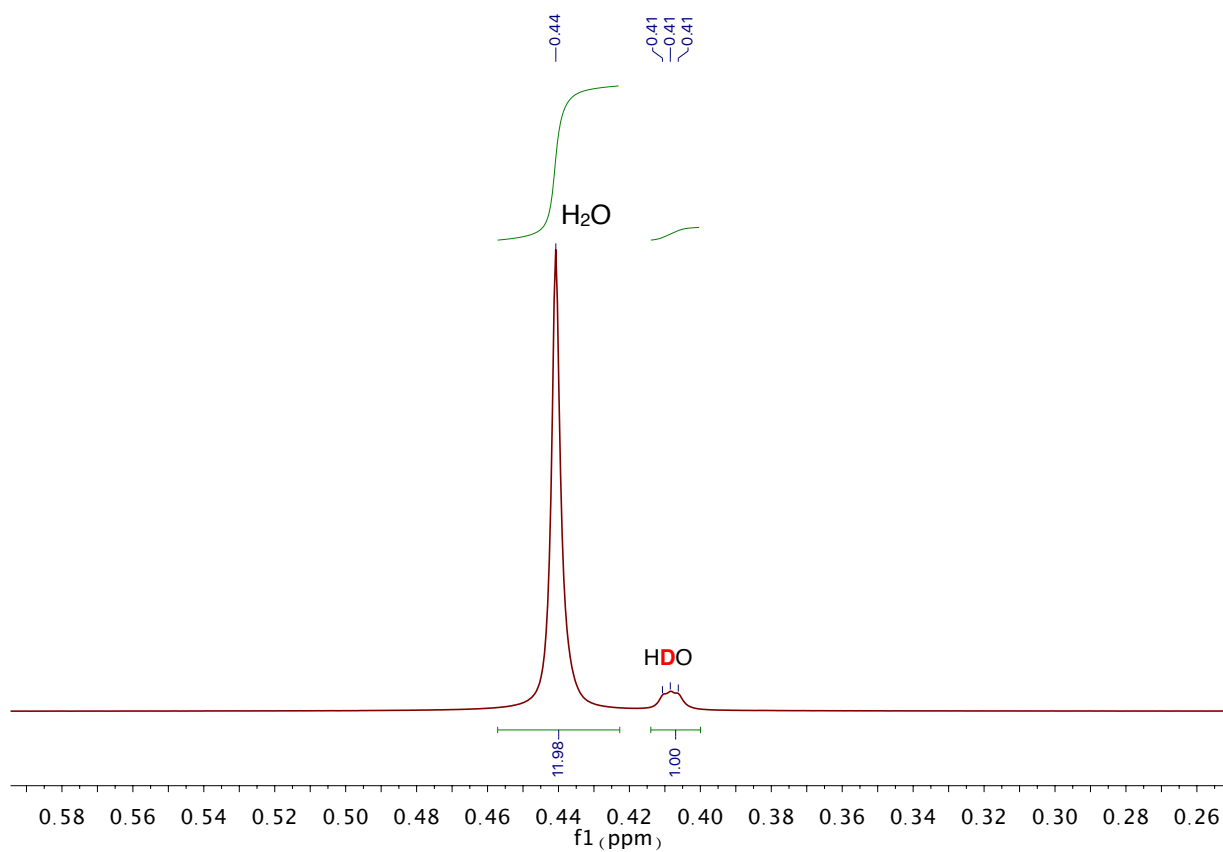
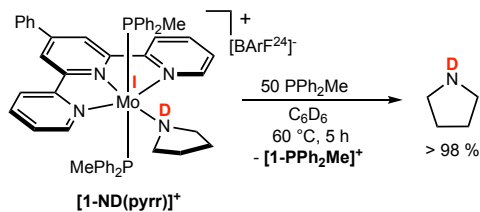


Figure S12. ^1H NMR spectrum (benzene- d_6 , 23 °C) of the captured combustion product following the dehydrogenation of pyrrolidine- $\text{N}-d_1$.



Displacement of Pyrrolidine Ligand from [1-ND(pyrr)]⁺. In the glovebox, a J-Young NMR tube fitted with a Teflon cap was charged with 0.030 g (0.017 mmol) of [1-ND(pyrr)]⁺, 0.160 mL (0.862 mmol) of PPh₂Me and 0.6 mL of benzene-*d*₆. The tube was sealed and connected to the high vacuum line where the solvent was de-gassed by 3x freeze-pump-thaw cycles. The tube was sealed and placed in a temperature-controlled oil bath (60 °C) for 5 hours. After this time, the volatiles of the reaction were vacuum distilled at 50°C into a second J-Young NMR tube fitted with a Teflon cap and analyzed by ²H and quantitative ¹³C{¹H} spectroscopies. Exclusively pyrrolidine-2-*d*₁ was observed.

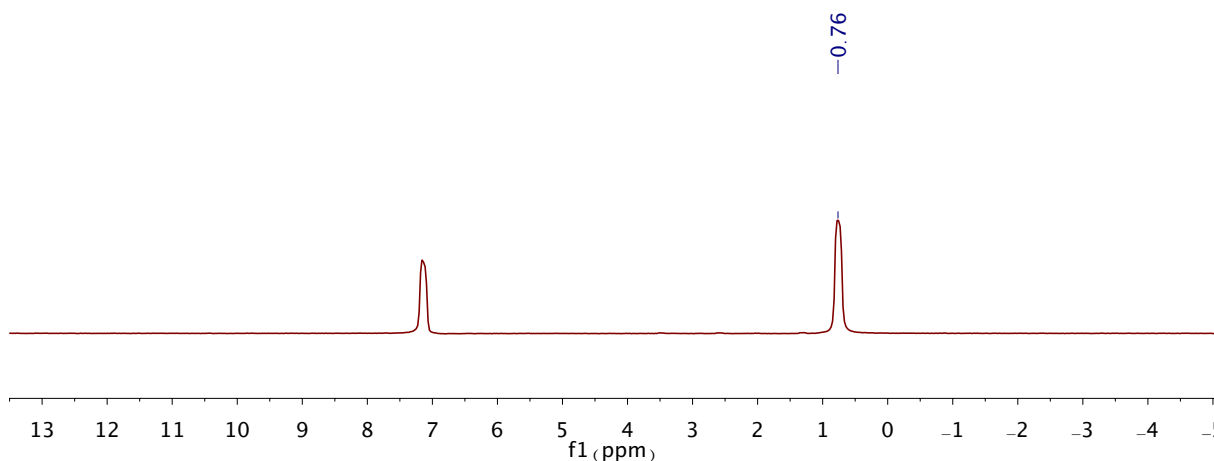


Figure S13. ²H NMR spectrum (benzene, 23 °C) of pyrrolidine-1-*d*₁ liberated from [1-ND(pyrr)]⁺.

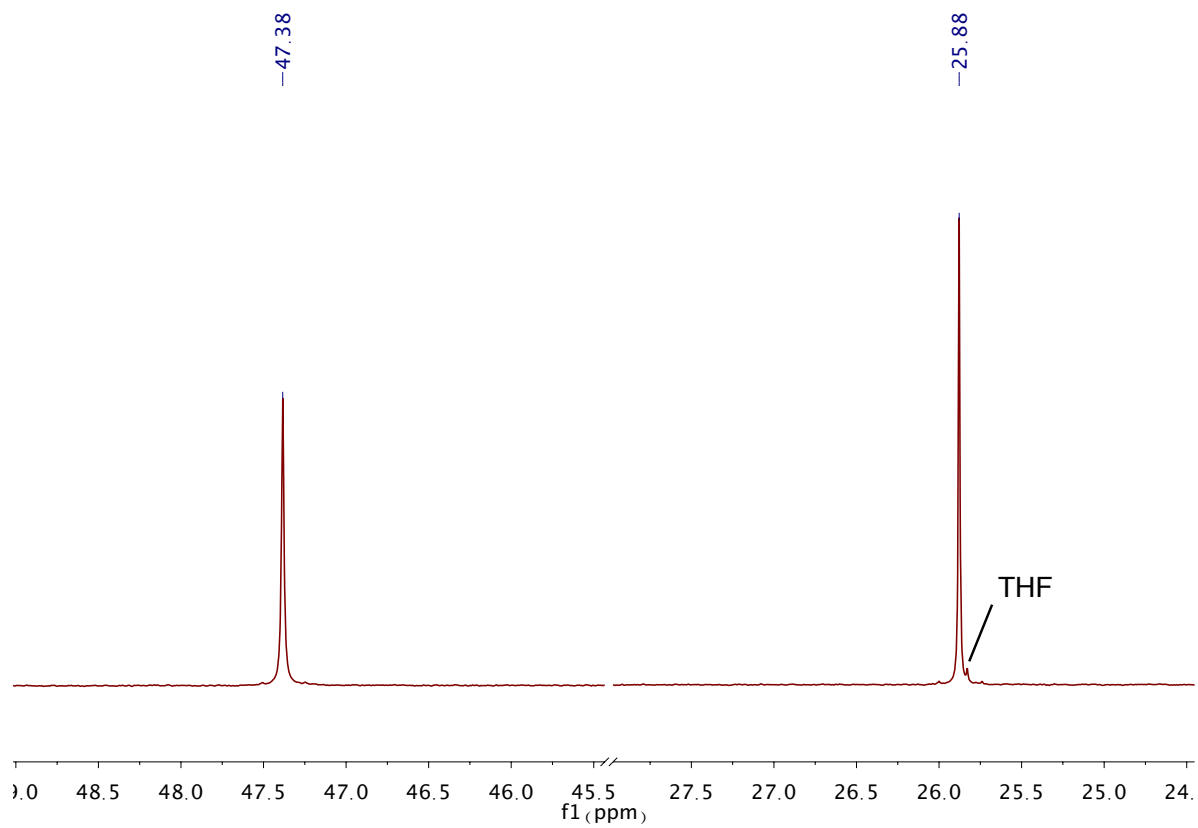
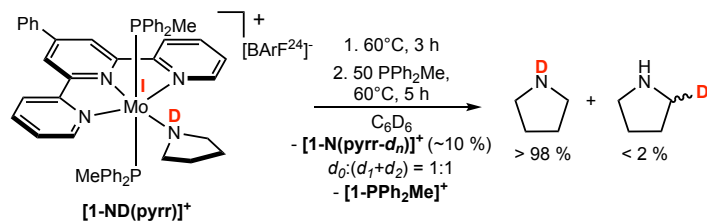


Figure S14. Quantitative $^{13}\text{C}\{^1\text{H}\}$ NMR spectrum (benzene- d_6 , 23 °C) of pyrrolidine-1- d_1 liberated from **[1-ND(pyrr)] $^+$** .



Displacement of Pyrrolidine Ligand from [1-ND(pyrr)]⁺ Following Partial Dehydrogenation. In the glovebox, a J-Young NMR tube fitted with a Teflon cap was charged with 0.025 g (0.014 mmol) of [1-ND(pyrr)]⁺ and 0.6 mL of benzene-*d*₆. The tube was sealed and connected to the high vacuum line where the solvent was de-gassed by 3x freeze-pump-thaw cycles. The tube was sealed and placed in a temperature-controlled oil bath (60 °C) for 3 hours. The tube was then brought back into the glovebox, where 0.134 mL (0.718 mmol) of PPh₂Me was added. The tube was sealed and connected to the high vacuum line where the solvent was de-gassed by 3x freeze-pump-thaw cycles. The tube was sealed and placed in a temperature-controlled oil bath (60 °C) for 5 hours. After this time, the volatiles of the reaction were vacuum distilled at 50°C into a second J-Young NMR tube fitted with a Teflon cap and analyzed by ²H and quantitative ¹³C{¹H} spectroscopies. Pyrrolidine-1-*d*₁ was observed (> 98%) with traces (< 2 %) of pyrrolidine-2-*d*₁.

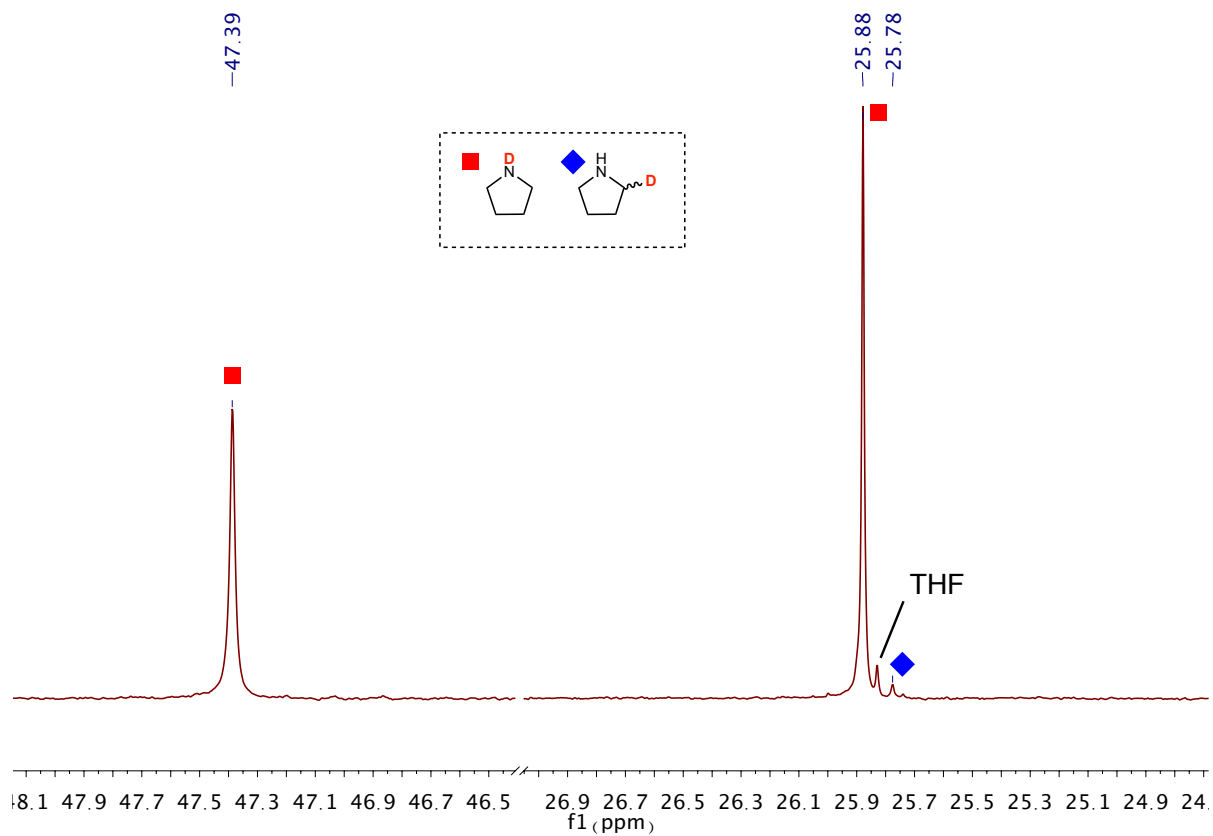
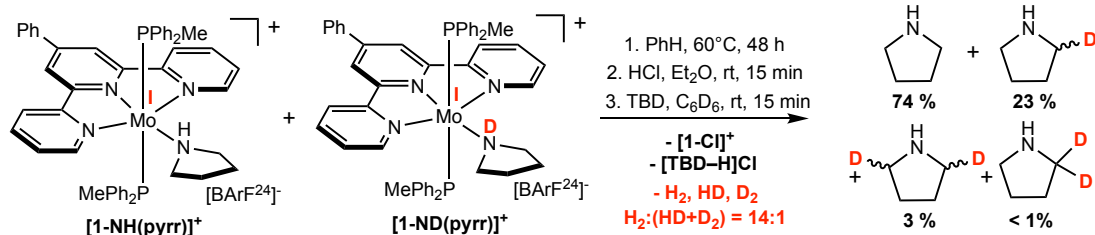


Figure S15. Quantitative $^{13}\text{C}\{^1\text{H}\}$ NMR spectrum (benzene- d_6 , 23 °C) of a mixture containing pyrrolidine-1- d_1 (> 98%) with traces (< 2 %) of pyrrolidine-2- d_1 liberated from **[1-ND(pyrr)] $^+$** after partial dehydrogenation.



Crossover Experiment between [1-NH(pyrr)]⁺ and [1-ND(pyrr)]⁺. In the glovebox, a J-Young NMR tube fitted with a Teflon cap was charged with 0.040 g (0.023 mmol) of [1-ND(pyrr)]⁺, 0.040 g (0.023 mmol) of [1-NH(pyrr)]⁺ and 0.6 mL of benzene-*d*₆. The tube was sealed and connected to the high vacuum line where the solvent was de-gassed by 3x freeze-pump-thaw cycles. The tube was sealed and placed in a temperature-controlled oil bath (60 °C) for 48 hours. A quantitative ¹³C{¹H} NMR spectrum was recorded after 3 hours (Figure S12) and after 48 hours (Figure S13) of stirring to monitor the isotopic composition of the pyrrolidide ligand in the molybdenum product. The tube was then brought back into the glovebox and product isolation was carried out as described for [1-N(pyrr)]⁺ (Method A). The isotopic composition of the evolved gases and the pyrrolidide ligand were determined as described above.

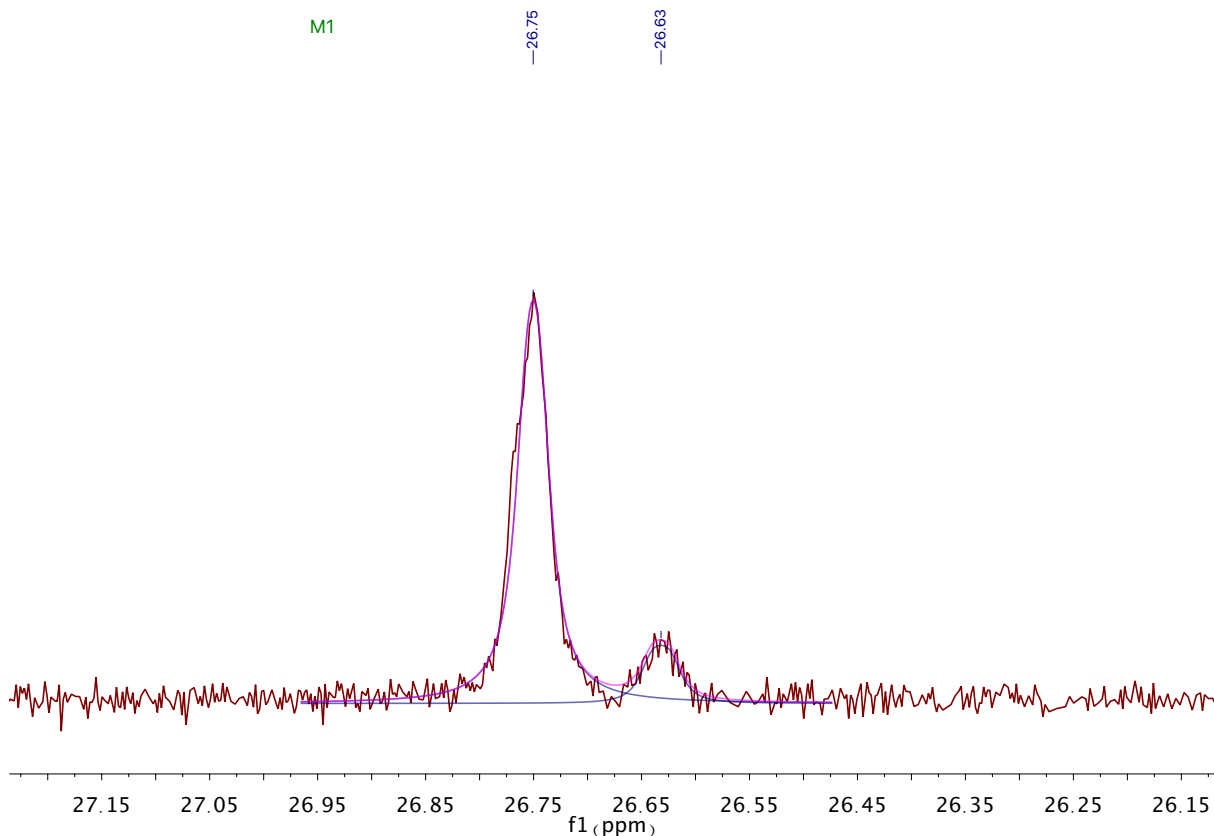


Figure S16. Fitted quantitative $^{13}\text{C}\{^1\text{H}\}$ NMR spectrum (benzene- d_6 , 23 °C) of the β -pyrrolidide region of the crossover experiment between $[\mathbf{1-NH(pyrr)}]^+$ and $[\mathbf{1-ND(pyrr)}]^+$ after heating at 60 °C for 3 hours. The violet line represents a fit of the data, and the blue lines shows the deconvolution of the individual peaks.

Table S2. Assignments and relative integrations of the peaks observed in Figure S12.

δ (multiplicity)	Assignment	Integration (MestReNova Curve Fit)
26.75 (s)	$[\mathbf{1-N(pyrr)}]^+$	116468.521
26.63 (s)	$[\mathbf{1-N(pyrr-d_1)}]^+$	16919.566

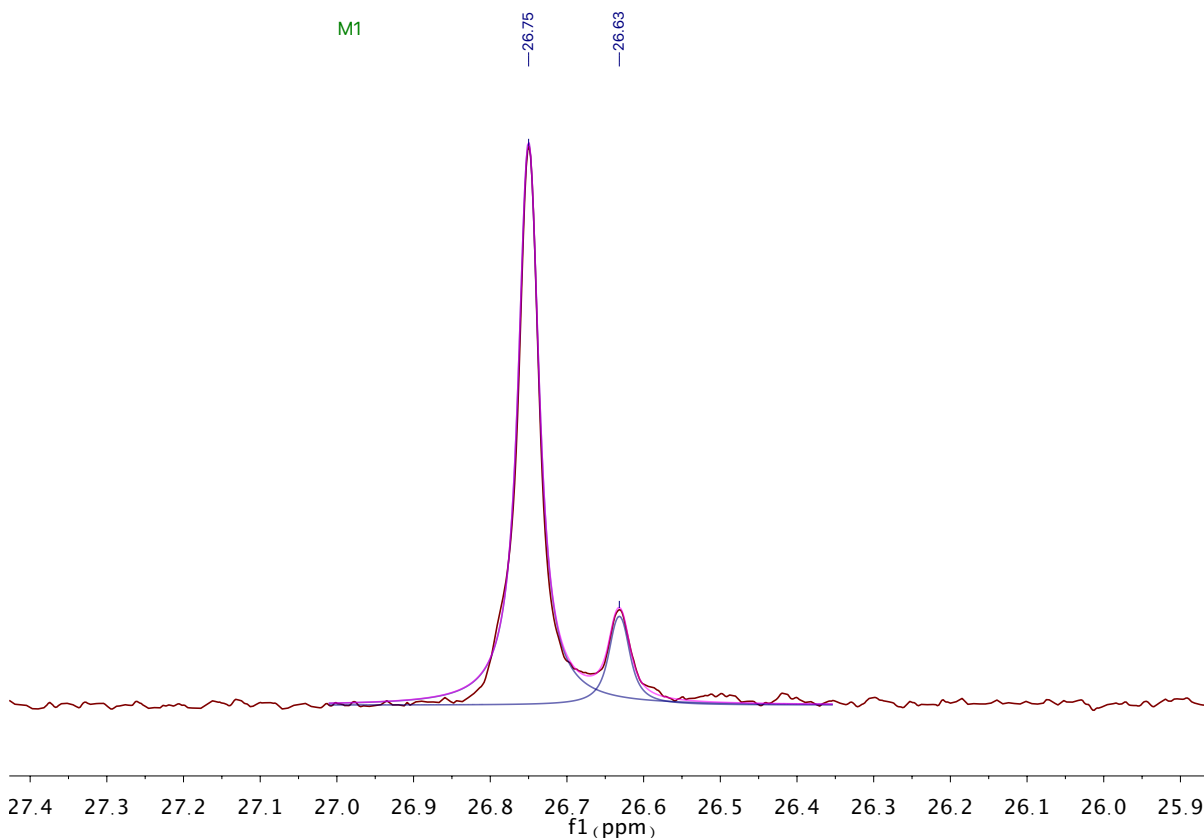


Figure S17. Fitted quantitative $^{13}\text{C}\{^1\text{H}\}$ NMR spectrum (benzene- d_6 , 23 °C) of the β -pyrrolidide region of the crossover experiment between **[1-NH(pyrr)]⁺** and **[1-ND(pyrr)]⁺** after heating at 60 °C for 3 hours. The violet line represents a fit of the data, and the blue lines shows the deconvolution of the individual peaks.

Table S3. Assignments and relative integrations of the peaks observed in Figure S13.

δ (multiplicity)	Assignment	Integration (MestReNova Curve Fit)
26.75 (s)	[1-N(pyrr)]⁺	164161.551
26.63 (s)	[1-N(pyrr-d_1)]⁺	24513.016

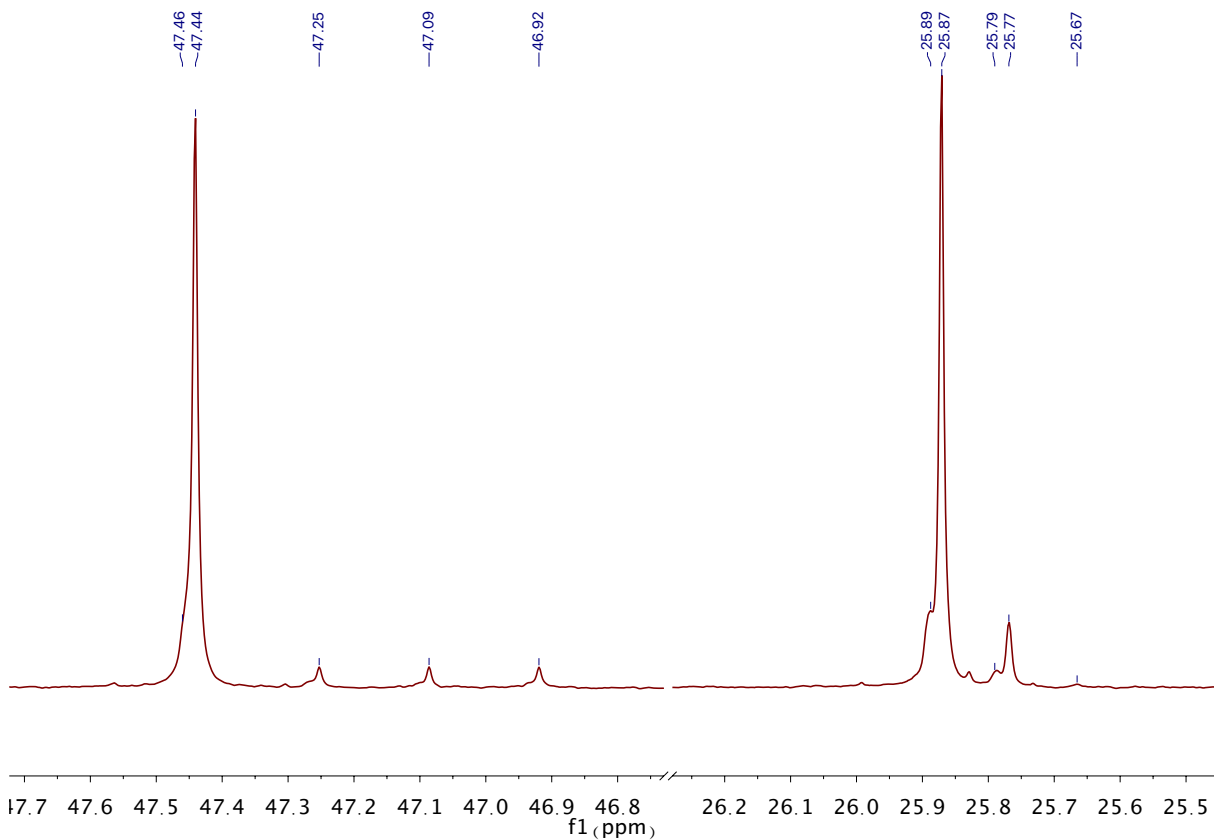


Figure S18. Quantitative $^{13}\text{C}\{^1\text{H}\}$ NMR spectrum (benzene- d_6 , 23 °C) of a mixture containing pyrrolidine (74 %), pyrrolidine-2- d_1 (23 %), pyrrolidine-2,5- d_1,d_1 (3 %) and pyrrolidine-2,2- d_2 (< 1 %) liberated from the product of the crossover experiment between **[1-NH(pyrr)]⁺** and **[1-ND(pyrr)]⁺**.

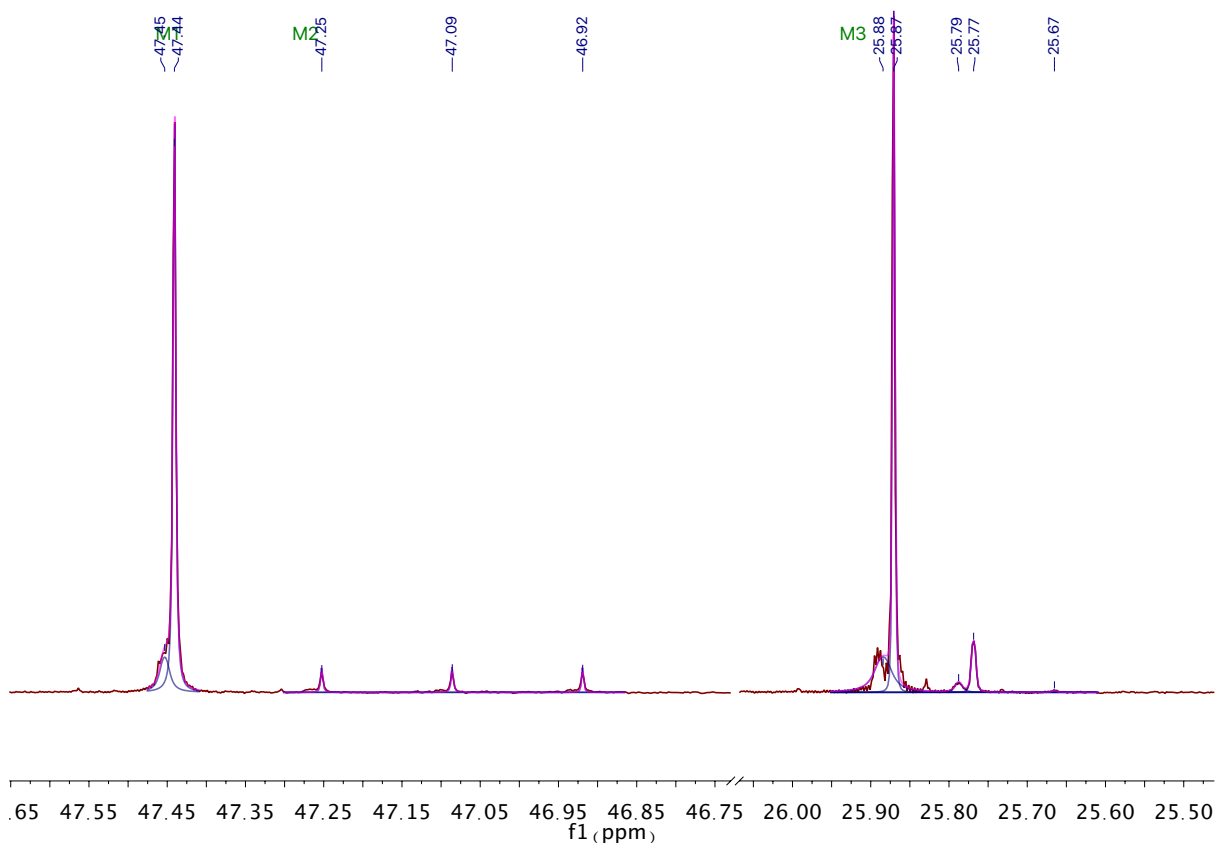
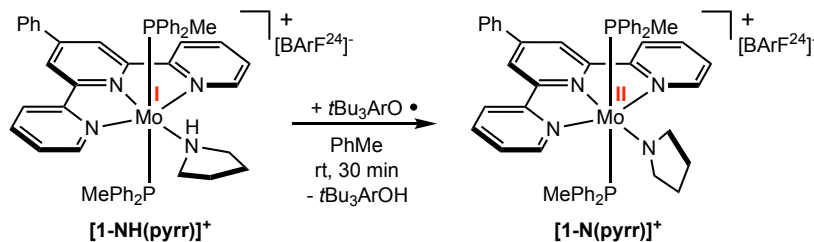
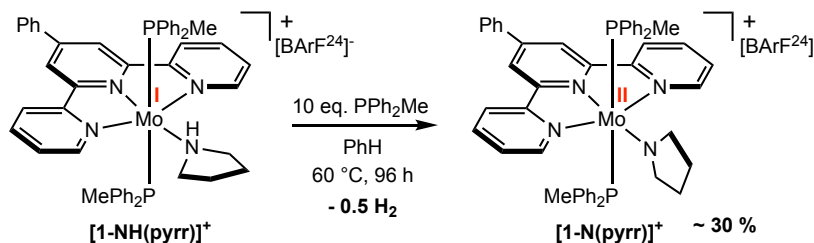


Figure S19. Fitted quantitative $^{13}\text{C}\{^1\text{H}\}$ NMR spectrum (benzene- d_6 , 23 °C) of a mixture containing pyrrolidine (74 %), pyrrolidine-2- d_1 (23 %), pyrrolidine-2,5- d_{1,d_1} (3 %) and pyrrolidine-2,2- d_2 (< 1 %) liberated from the product of the crossover experiment between $[\mathbf{1-NH(pyrr)}]^+$ and $[\mathbf{1-ND(pyrr)}]^+$. Data was processed with low exponential apodization (0.2 Hz) to better resolve isotopolog/isotopomer peaks. The violet line represents a fit of the data, and the blue lines shows the deconvolution of the individual peaks. For individual peak assignments see Table S1.

V. Additional Reactions and Associated NMR Data



PCET reaction between [1-NH(pyrr)]⁺ and tBu₃ArO•. In the glovebox, a 20 mL scintillation vial was charged with a magnetic stir bar, 0.038 g (0.022 mmol) of [1-NH(pyrr)]⁺ and 2 mL of toluene. To the stirring solution, 0.006 g (0.023 mmol) of tBu₃ArO• dissolved in 0.5 mL of toluene was added dropwise. During the addition, a color change from dark green to brown was observed, and the solution was stirred at room temperature for an additional 30 minutes. The solvent was then removed *in vacuo*, and the quantitative formation of [1-N(pyrr)]⁺ and tBu₃ArOH was observed by ¹H NMR spectroscopy (vs mesitylene internal standard).



Thermolysis of [1-NH(pyrr)]⁺ in the presence of excess PPh₂Me. In the glovebox, a J-Young NMR tube fitted with a Teflon cap was charged with 0.028 g (0.016 mmol) of [1-NH(pyrr)]⁺, 0.030 mL (0.161 mmol) of PPh₂Me and 0.6 mL of benzene-*d*₆. The tube was sealed and placed in a temperature-controlled oil bath (60 °C) and monitored by ¹H and ³¹P{¹H} spectroscopies.

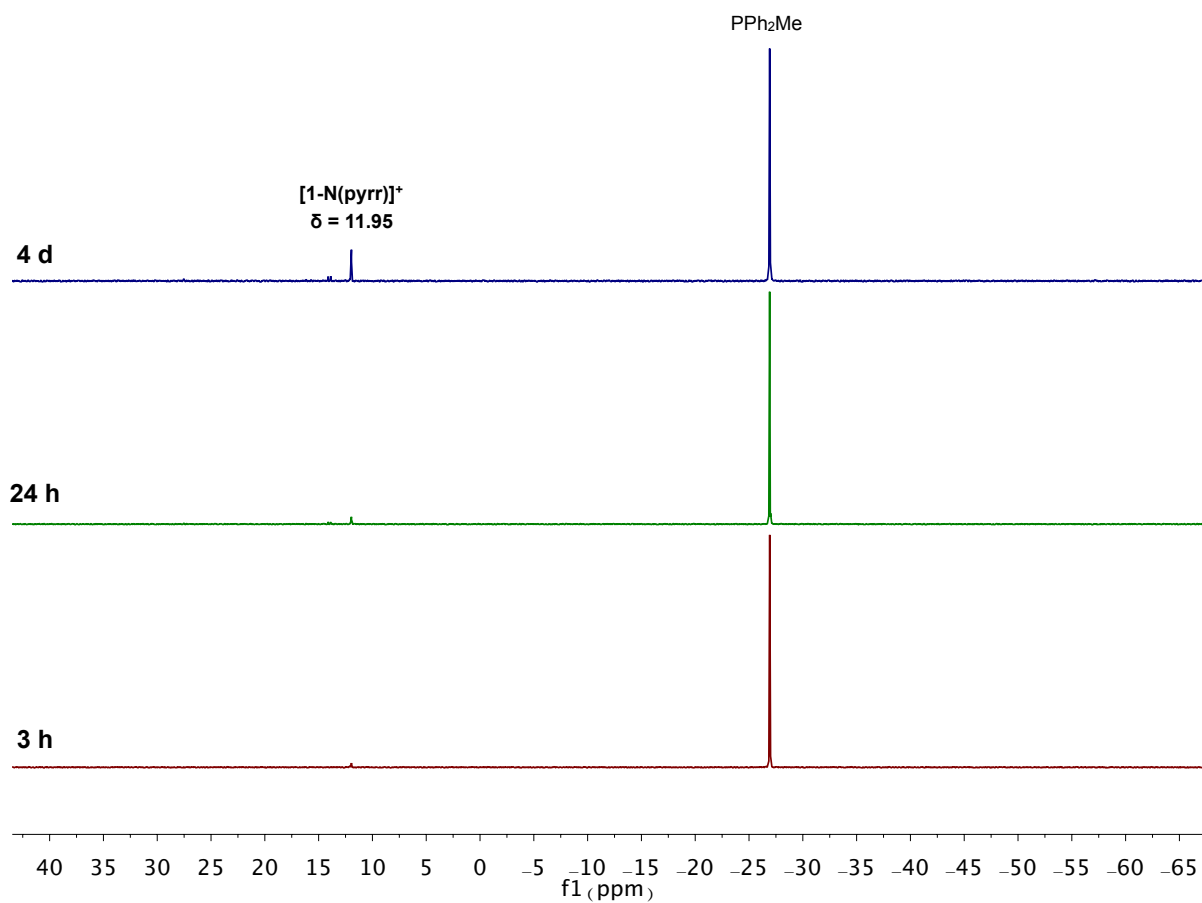
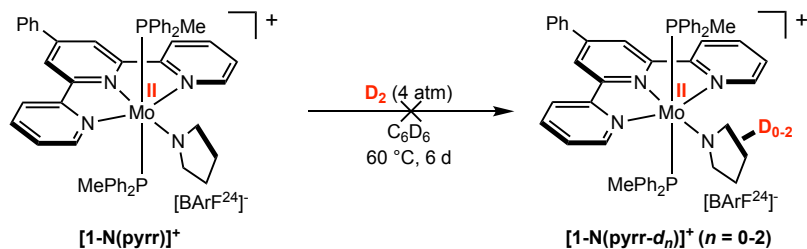


Figure S20. $^{31}\text{P}\{^1\text{H}\}$ spectra taken at various intervals during the thermolysis $[\text{1-NH(pyrr)}]^+$ in the presence of 10 equiv. of PPh_2Me . The 4 day mark represents $\sim 30\%$ yield.



Reaction of [1-N(pyrr)]⁺ with D₂. In the glovebox, a J-Young NMR tube fitted with a Teflon cap was charged with 0.026 g (0.015 mmol) of [1-N(pyrr)]⁺, and 0.6 mL of benzene-*d*₆. The tube was sealed and connected to the high vacuum line where the headspace was evacuated and D₂ (4 atm) was admitted. The tube was sealed and placed in a temperature-controlled oil bath (60 °C) for 5 days. After this time, a quantitative ¹³C{¹H} NMR spectrum was recorded and showed no deuterium incorporation in the pyrroldide ligand.

VI. Additional Spectroscopic Data

VI. A. EPR Spectra

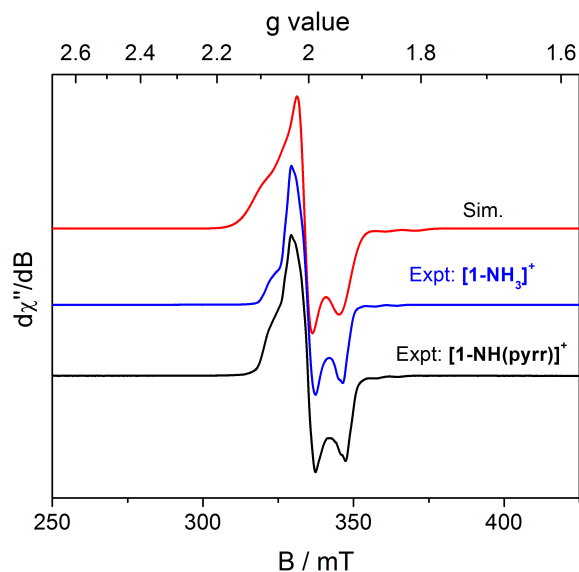


Figure S21. Overlaid X-band EPR spectra of **[1-NH(pyrr)]⁺** (black), **[1-NH₃]⁺** (blue) recorded at 7 K in toluene glass and a fit of the data (red). Collection and simulation parameters: microwave frequency = 9.381 GHz, power = 2.0 mW, modulation amplitude = 4.0 G; $g_x = 2.020$, $g_y = 2.005$, $g_z = 1.968$.

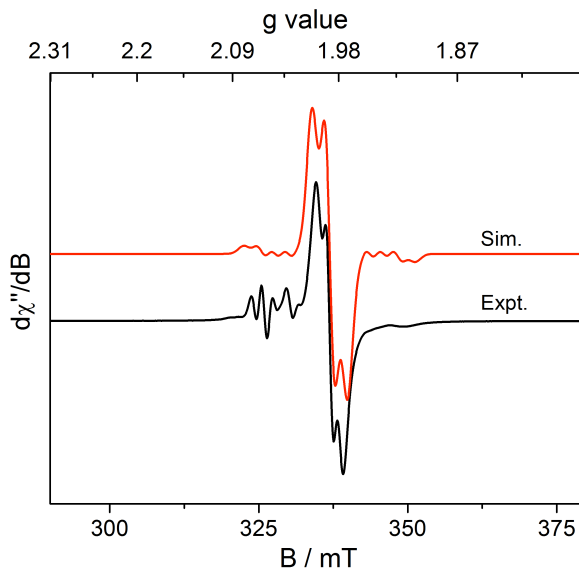


Figure S22: X-band EPR spectrum of **[1-NH(pyrr)]⁺** (black) recorded at 296 K in toluene solution and a fit of the data (red). Collection and simulation parameters: microwave frequency = 9.378 GHz, power = 2.0 mW, modulation amplitude = 4.0 G; $g_{\text{iso}} = 1.989$, g_{iso} strain = 0.007, $A_{\text{iso}}(^{95/97}\text{Mo}) = 63$ MHz (assuming 15.92% naturally occurring ^{95}Mo with $I = 5/2$ and 9.55% naturally occurring ^{97}Mo with $I = 5/2$), $A_{\text{iso}}(^{31}\text{P}) = 29$ MHz (assuming 100% naturally occurring ^{31}P nuclei with $I = 1/2$).

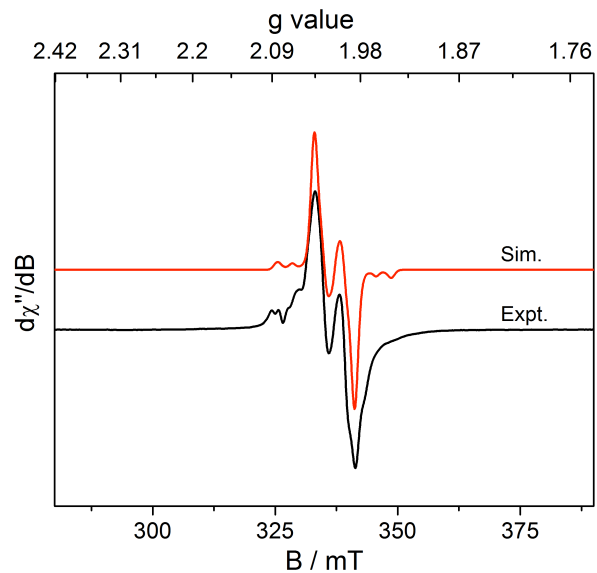


Figure S23: X-band EPR spectrum of **[1-PPh₂Me]⁺** (black) recorded at 296 K in toluene solution and a fit of the data (red). Collection and simulation parameters: microwave frequency = 9.488 GHz, power = 2.0 mW, modulation amplitude = 4.0 G; $g_{\text{iso}} = 2.011$, g_{iso} strain = 0.005, A_{iso} (^{95/97}Mo) = 42 MHz (assuming 15.92% naturally occurring ⁹⁵Mo with $I = 5/2$ and 9.55% naturally occurring ⁹⁷Mo with $I = 5/2$), A_{iso} (³¹P) = 58 MHz, 27 MHz, 15 MHz (assuming 100% naturally occurring ³¹P nuclei with $I = 1/2$).

VI. B. IR Spectra

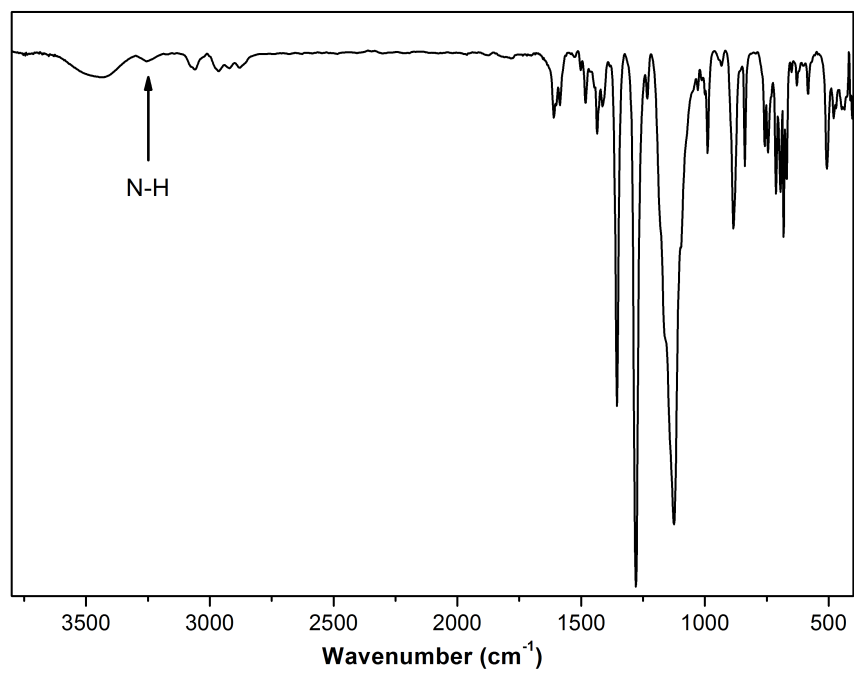


Figure S24. IR spectrum of **[1-NH(pyrr)]⁺** recorded at 296 K in a KBr pellet.

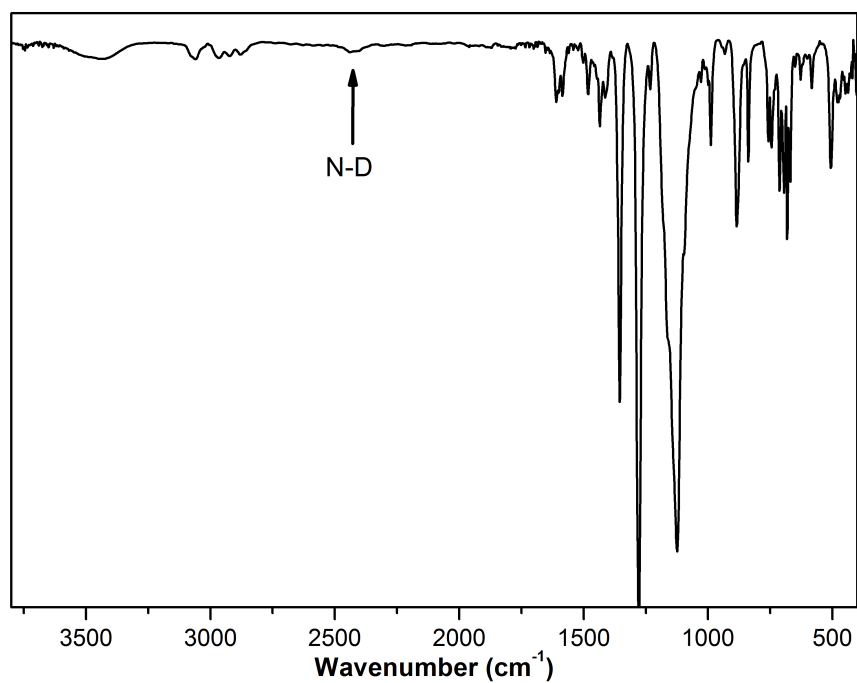
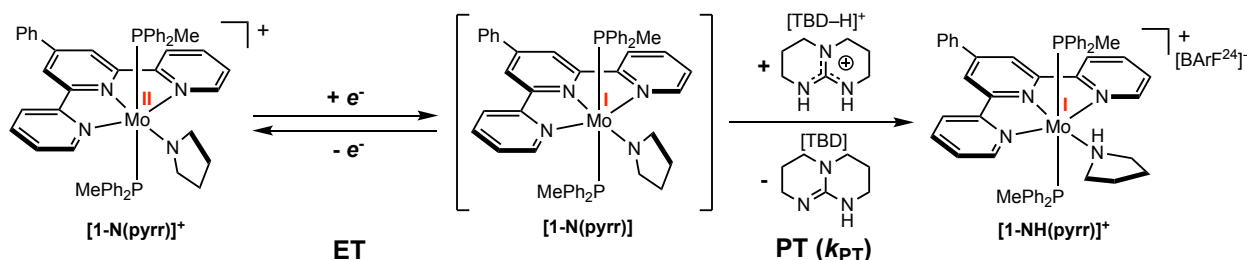


Figure S25. IR spectrum of **[1-ND(pyrr)]⁺** recorded at 296 K in a KBr pellet.

VII. Electrochemical Determination of k_{PT} between [1-N(pyrr)] and [TBD-H][BARF²⁴]

We assume that an electron transfer (ET) event is followed by a rapid, irreversible proton transfer (PT) between [1-N(pyrr)] and [TBD-H][BARF²⁴] in the electrochemical cell:



In this case, the observed rate constant for the chemical step (proton transfer) can be expressed as:

$$k_{obs} = k_{PT}[TBD-H]$$

Where k_{PT} is the second-order rate constant for proton transfer and [TBD-H] is the concentration of the acid. It has been shown¹⁸ that the peak cathodic potential of the ET event varies as a function of acid concentration according to:

$$E_p = E_{1/2} - 0.78 \frac{RT}{F} + \frac{RT}{2F} \ln \left(\frac{k_{obs}RT}{Fv} \right)$$

Where E_p = Peak cathodic potential; $E_{1/2}$ = Potential of cathodic wave in the absence of acid; R = gas constant; T = temperature; F = Faraday's constant; v = scan rate.

Therefore, plotting the peak potential (E_p) as a function of $\ln([TBD-H]^+)$ allows the determination of k_{obs} and by extension, k_{PT} .

VIII. DFT Input Examples

VIII. A. Geometry Optimizations

#Filename

```
! RKS B3LYP RIJCOSX ZORA ZORA-def2-SVP SARC/J Normalprint SlowConv  
TightSCF Opt Pal8 UCO
```

```
%basis NewGTO 42 "old-ZORA-TZVP" end  
      NewGTO 15 "ZORA-DEF2-TZVP(-f)" end  
      NewGTO 7 "ZORA-DEF2-TZVP(-f)" end  
      NewAuxGTO 42 "SARC/J" end  
      NewAuxGTO 15 "SARC/J" end  
      NewAuxGTO 7 "SARC/J" end  
      end
```

```
%SCF MaxIter 500  
      TolE 1e-7  
      TolErr 1e-6  
      end
```

```
* xyz 1 1
```

XYZ Coordinates.

*

VIII. B. Numerical Frequency Calculations

```
#Filename  
! RKS B3LYP RIJCOSX SlowConv TightSCF ZORA ZORA-def2-SVP SARC/J  
Normalprint Numfreq Grid4 Nofinalgrid Pal8
```

```
%basis NewGTO 42 "old-ZORA-TZVP" end  
  NewGTO 7 "ZORA-DEF2-TZVP(-f)" end  
  NewGTO 15 "ZORA-DEF2-TZVP(-f)" end  
  NewAuxGTO 42 "SARC/J" end  
  NewAuxGTO 7 "SARC/J" end  
  NewAuxGTO 15 "SARC/J" end  
end
```

```
%SCF MaxIter 500  
  TolE 1e-7  
  TolErr 1e-6  
end
```

```
%FREQ RESTART TRUE  
CENTRALDIFF TRUE  
INCREMENT 0.01  
END
```

```
* xyz 1 1
```

XYZ Coordinates from geometry optimization.

```
*
```

IX. DFT-Computed Energies of Complexes

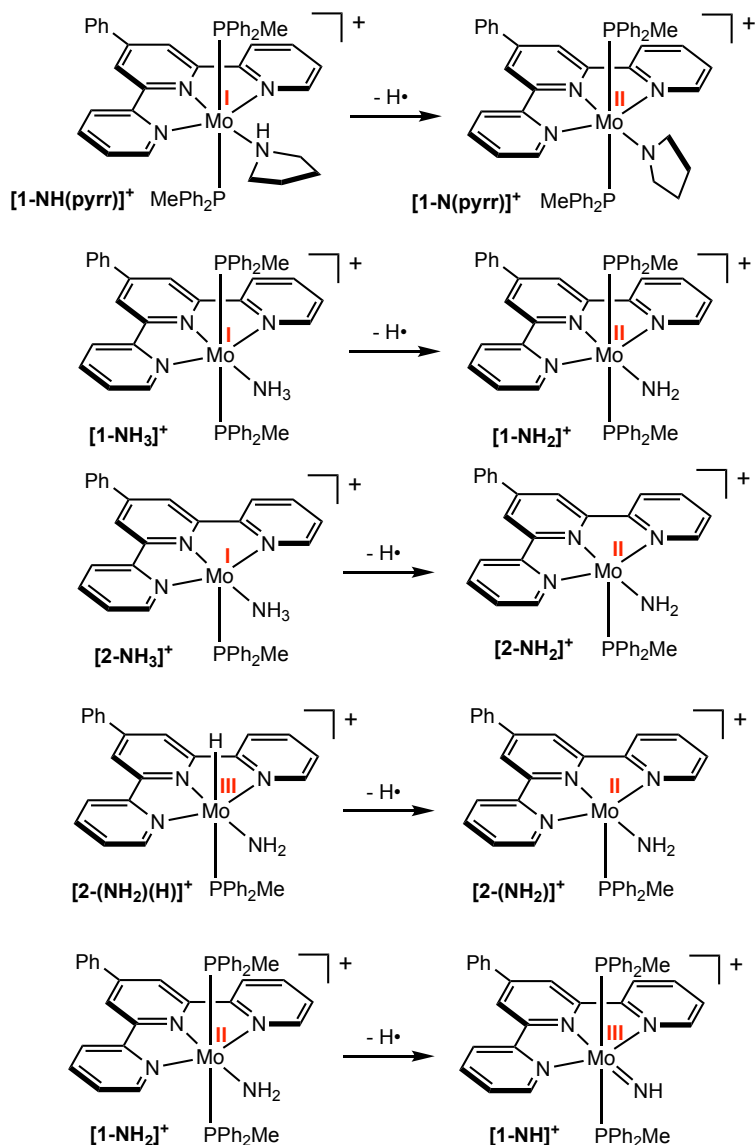


Table S4. Calculated Gibbs free energies of molybdenum complexes for N–H BDFE determinations.

Compound	Spin State	Calculated Gibbs Free Energy (Eh)
$[1\text{-NH(pyrr)}]^+$	$S = 1/2$	-6963.71188352
$[1\text{-N(pyrr)}]^+$	$S = 0$	-6963.13663953
$[1\text{-NH}_3]^+$	$S = 1/2$	-6807.89698148
$[1\text{-NH}_2]^+$	$S = 0$	-6807.32504940
$[2\text{-NH}_3]^+$	$S = 1/2$	-5962.56661616
$[2\text{-NH}_2]^+$	$S = 0$	-5961.99470463
$[2\text{-(NH}_2\text{)(H)}]^+$	$S = 1/2$	-5962.56799735
$[1\text{-NH}]^+$	$S = 1/2$	-6806.71994244

X. References

- 1 Pangborn, A. B.; Giardello, M. A.; Grubbs, R. H.; Rosen, R. K.; Timmers, F. J. Safe and Convenient Procedure for Solvent Purification. *Organometallics* **1996**, *15*, 1518–1520.
- 2 Bezdek, M. J.; Guo, S.; Chirik, P. J. Terpyridine Molybdenum Dinitrogen Chemistry: Synthesis of Dinitrogen Complexes That Vary by Five Oxidation States. *Inorg. Chem.* **2016**, *55*, 3117–3127.
- 3 Yakelis, N. A.; Bergman, R. G. Safe Preparation and Purification of Sodium Tetrakis[(3,5-trifluoromethyl)phenyl]borate (NaBARF₂₄): Reliable and Sensitive Analysis of Water in Solutions of Fluorinated Tetraarylborates. *Organometallics* **2005**, *24*, 3579.
- 4 Manner, V. W.; Markle, T. F.; Freudenthal, J. H.; Roth, J. P.; Mayer, J. M. The first crystal structure of a monomeric phenoxyl radical: 2,4,6-tri-*tert*-butylphenoxyl radical. *Chem. Commun.* **2008**, 256–258.
- 5 Soper, J. D.; Saganic, E.; Weinberg, D.; Hrovat, D. A.; Benedict, J. B.; Kaminsky, W.; Mayer, J. M. Nucleophilic Aromatic Substitution on Aryl-Amido Ligands Promoted by Oxidizing Osmium(IV) Centers. *Inorg. Chem.* **2004**, *43*, 5804–5815.
- 6 Xu, J.; Liu, J.; Li, Z.; Wang, H.; Xu, S.; Guo, T.; Zhu, H.; Wei, F.; Zhu, Y.; Guo, K. Guanidinium as bifunctional organocatalyst for ring-opening polymerizations. *Polymer* **2018**, *154*, 17–26.
- 7 Stoll, S.; Schweiger, A. EasySpin, a comprehensive software package for spectral simulation and analysis in EPR. *J. Magn. Reson.* **2006**, *178*, 42–55.
- 8 Neese, F. The ORCA program system. *Wiley Interdiscip. Rev.: Comput. Mol. Sci.* **2012**, *2*, 73–78.
- 9 (a) Becke, A. D. Density functional calculations of molecular bond energies. *J. Chem. Phys.* **1986**, *84*, 4524–4529. (b) Becke, A. D. Density-functional thermochemistry. III. The role of exact exchange. *J. Chem. Phys.* **1993**, *98*, 5648–5652. (c) Lee, C. T.; Yang, W. T.; Parr, R. G. Development of the Colle-Salvetti correlation-energy formula into a functional of the electron density. *Phys. Rev. B.* **1998**, *37*, 785–789.
- 10 (a) Schäfer, A.; Horn, H.; Ahlrichs, R. Fully optimized contracted Gaussian basis sets for atoms Li to Kr. *J. Chem. Phys.* **1992**, *97*, 2571–2577. (b) Schäfer, A.; Huber, C.; Ahlrichs, R. Fully optimized contracted Gaussian basis sets of triple zeta valence quality for atoms Li to Kr. *J. Chem. Phys.* **1994**, *100*, 5829–5835. (c) Weigend, F.; Ahlrichs, R. Balanced basis sets of split valence, triple zeta valence and quadruple zeta valence quality for H to Rn: Design and assessment of accuracy. *Phys. Chem. Chem. Phys.* **2005**, *7*, 3297–3305.
- 11 (a) Neese, F.; Wennmohs, F.; Hansen, A.; Becker, U. Efficient, Approximate and parallel Hartree–Fock and hybrid DFT calculations. A ‘chain-of-spheres’ algorithm for the Hartree–Fock exchange. *Chem. Phys.* **2009**, *356*, 98–109. (b) Kossmann, S.; Neese, F. Comparison of two efficient approximate Hartree–Fock approaches. *Chem. Phys. Lett.*

- 2009**, 481, 240–243. (c) Neese, F. An improvement of the resolution of the identity approximation for the formation of the Coulomb matrix. *J. Comput. Chem.* **2003**, 24, 1740–1747.
- 12 (a) Eichkorn, K.; Weigend, F.; Treutler, O.; Ahlrichs, R. Auxiliary basis sets for main row atoms and transition metals and their use to approximate Coulomb potentials. *Theor. Chem. Acc.* **1997**, 97, 119–124. (b) Eichkorn, K.; Treutler, O.; Öhm, H.; Häser, m.; Ahlrichs, R. Auxiliary basis sets to approximate Coulomb potentials. *Chem. Phys. Lett.* **1995**, 240, 283–289. (c) Eichkorn, K.; Treutler, O.; Öhm, H.; Häser, M.; Ahlrichs, R. Auxiliary basis sets to approximate Coulomb potentials. *Chem. Phys. Lett.* **1995**, 242, 652–660.
- 13 van Wullen, C. Molecular density functional calculations in the regular relativistic approximation: Method, application to coinage metal diatomics, hydrides, fluorides and chlorides, and comparison with first-order relativistic calculations. *J. Chem. Phys.* **1998**, 109, 392–399.
- 14 Weigend, F.; Ahlrichs, R. Balanced basis sets of split valence, triple zeta valence and quadruple zeta valence quality for H to Rn: Design and assessment of accuracy. *Phys. Chem. Chem. Phys.* **2005**, 7, 3297–3305.
- 15 Beak, P.; Kerrick, S. T.; Wu, S.; Chu, J. Complex Induced Proximity Effects: Enantioselective Syntheses Based on Asymmetric Deprotonations of *N*-Boc-pyrrolidines. *J. Am. Chem. Soc.* **1994**, 116, 3231–3239.
- 16 Bezdek, M. J.; Chirik, P. J. Proton-Coupled Electron Transfer to a Molybdenum Ethylene Complex Yields a β -Agostic Ethyl: Structure, Dynamics and Mechanism. *J. Am. Chem. Soc.* **2018**, 140, 13817–13826.
- 17 Pyper, J. W.; Newbury, R. S.; Barton, G. W. Study of the Isotopic Disproportionation Reaction between Light and Heavy Water Using a Pulsed-Molecular-Beam Mass Spectrometer. *J. Chem. Phys.* **1967**, 46, 2253–2257.
- 18 (a) Savéant, J.-M. *Elements of Molecular and Biomolecular Electrochemistry*; John Wiley & Sons: Hoboken, NJ, **2006**; (b) Elgrishi, N.; Kurtz, D. A.; Dempsey, J. L. Reaction Parameters Influencing Cobalt Hydride Formation Kinetics: Implications for Benchmarking H₂-Evolution Catalysts. *J. Am. Chem. Soc.* **2017**, 139, 239–244.